

MASSACHUSETTS INSTITUTE OF TECHNOLOGY

APOLLO

GUIDANCE, NAVIGATION AND CONTROL

E-2543

ELIMINATION OF NOISE AND
ENHANCEMENT OF STABILITY AND
DYNAMIC RESPONSE OF THE APOLLO LM
RATE-OF-DESCENT PROGRAM

by
A. KLUMPP
G. KALAN

OCTOBER 1970

MIT

CAMBRIDGE MASSACHUSETTS 02139

**CHARLES STARK DRAPER
LABORATORY**



GUIDANCE, NAVIGATION AND CONTROL

Approved: Donald C. Fraser Date: 27 Oct 1970
D. C. FRASER, DIR., CONTROL AND FLIGHT DYNAMICS
APOLLO GUIDANCE AND NAVIGATION PROGRAM

Approved: Gerald M. Levine Date: 22 Oct 70
G. M. LEVINE, DIRECTOR, GUIDANCE ANALYSIS
APOLLO GUIDANCE AND NAVIGATION PROGRAM

Approved: R. H. Battin Date: 29 Oct 70
R. H. BATTIN, DIRECTOR, MISSION DEVELOPMENT
APOLLO GUIDANCE AND NAVIGATION PROGRAM

Approved: D. G. Hoag Date: 30 Oct 70
D. G. HOAG, DIRECTOR
APOLLO GUIDANCE AND NAVIGATION PROGRAM

Approved: Ralph R. Ragan Date: 30 Oct 70
R. R. RAGAN, DEPUTY DIRECTOR
CHARLES STARK DRAPER LABORATORY

E-2543

ELIMINATION OF NOISE AND
ENHANCEMENT OF STABILITY AND
DYNAMIC RESPONSE OF THE APOLLO LM
RATE-OF-DESCENT PROGRAM

by
A. KLUMPP
G. KALAN

OCTOBER 1970



CHARLES STARK DRAPER
LABORATORY

CAMBRIDGE, MASSACHUSETTS, 02139

ACKNOWLEDGEMENT

This report was prepared under DSR Project 55-23890, sponsored by the Manned Spacecraft Center of the National Aeronautics and Space Administration through Contract NAS 9-4065.

The publication of this report does not constitute approval by the National Aeronautics and Space Administration of the findings or the conclusions contained therein. It is published only for the exchange and stimulation of ideas.

ELIMINATION OF NOISE AND ENHANCEMENT OF STABILITY AND
DYNAMIC RESPONSE OF THE APOLLO LUNAR MODULE
RATE OF DESCENT PROGRAM

ABSTRACT

At about 30 ft. altitude in the Apollo 12 Lunar descent, unexpected excursions of the lunar module descent propulsion system throttle occurred. The excitation initiating the throttle excursions was found to be several sudden pitch attitude corrections performed manually with the attitude control assembly (ACA) by Commander Charles (Pete) Conrad. Because the inertial measurement unit (IMU) is located substantially in front of the center of mass of the LM, these pitch rates produced IMU bobbing motions which were detected by the vertically sensing accelerometer. The IMU bobbing motions caused the guidance program to compute apparent thrust and altitude rate changes and consequently to command the unnecessary throttle excursions. In addition, a deficiency in the damping of the guidance and control system was indicated by the persistence of throttle excursions following the initial excitation. The damping deficiency was traced to a mismatch between the actual time constant of the descent engine and the time constant assumed by the guidance and control compensation. The excitation has been eliminated for Apollo 14 by correcting the accelerometer readings such that the readings are referred to the center of mass of the LM. The damping of the guidance and control loops has been enhanced by matching the compensation to the measured performance of the descent engine. Digital simulations of the LM descent, which include attitude excitations similar to those of Apollo 12, have been made using the corrected system. A parameter sensitivity study has been performed

using a Z transform model of the system to determine the stability limits. These limits have been verified by digital simulation. The Z transform analysis and digital simulation study indicate that the excitation has been eliminated, the system is correctly modeled and compensated, and the stability margins are adequate.

by: Allan Klumpp and George Kalan

October 1970

TABLE OF CONTENTS

	PAGE
NOMENCLATURE -----	1
INTRODUCTION -----	5
EXCITATION ELIMINATION -----	7
STABILITY ENHANCEMENT -----	9
Model -----	9
Parameter Settings -----	11
Stability Margins -----	12
CONCLUSIONS -----	15
FIGURE 1 LM Geometry Responsible for Exciting the ROD Guidance with Pitch Rates -----	16
FIGURE 2 Apollo 12 and Bit-by-Bit Simulator Response to Pitch Rates	17
FIGURE 3 Response to Attitude and Altitude Rate Inputs for Various ROD Parameters with Accelerometer Readings not Referred to the Center of Mass -----	18
FIGURE 4 Response to Attitude and Altitude Rate Inputs for Various ROD Parameters with Accelerometer Readings Referred to the Center of Mass -----	19
FIGURE 5 ROD Guidance Channel Linearized Block Diagram -----	20
FIGURE 6 ROD Guidance Channel Reduced Linearized Block Diagram -	21
FIGURE 7 ROD Guidance Channel Reduced Z Transform Diagram -----	22
FIGURE 8 Performance and roots for proposed Apollo 14 ROD parameters -----	23
TABLE 1 Stability Regions for each Parameter Determined with Z Transform Analysis-----	24

	PAGE
FIGURES 9-14 Performance and Roots vs. System Parameters-----	25
FIGURES 15-26 Performance and Roots at System Parameter Extremes -----	31
REFERENCES -----	43
APPENDIX A Derivation of the Acceleration Correction Increment	45
FIGURE A1 Acceleration Response Model Used in Deriving the Acceleration Correction Increment δA_p -----	47
APPENDIX B Pole-Zero Polynomial Coefficients -----	49
TABLE B1 Coefficients of the Closed Loop System Poles and Zeros with the Engine Modeled as a First Order Lag-----	51
TABLE B2 Coefficients of the Closed Loop System Poles and Zeros with the Engine Modeled as a Pure Time Delay -----	52
FIGURE B1 Performance and roots for pole-zero cancellation	53
APPENDIX C Conditions for Bit-by-Bit Simulations -----	55
APPENDIX D Analysis of Faster Systems -----	59
TABLE D1 Stability Regions of Each Parameter for TAUROD = 1.2 -----	60
FIGURES D1-D5 Performance and Roots vs. System Para- meters for TAUROD = 1.2 -----	61
TABLE D2 Stability Regions of Each Parameter for TAUROD = 1.0 -----	66
FIGURES D6 -D10 Performance and Roots vs. System Para- meters for TAUROD = 1.0 -----	67

NOMENCLATURE

Several systems of nomenclature are used in connection with the ROD guidance program. The following table provides a cross reference between these nomenclatures.

THIS MEMO	ABBREVIATION	LGC	GSOP (Ref. 4)
TAUROD	TV	TAUROD	TAUROD
LAG	L	LAG	LAG
LAG/TAU	-	LAG/TAU	Lag/TAUROD
THROTLAG	TT	THROTLAG	τ_{th}
TAUENG	TE	-	-
DELAY	D	P PROCESS + $ PIF /(2 FRATE)$	$t_{fc} - t_n +$ $ f - \tilde{f} /(2 FRATE)$
KFM	KFM	-	-
δA_P	δA_P	FWEIGHT	δf_P Note 1

Note 1: δA_P is equivalent to δf_P and FWEIGHT although δA_P has acceleration units and δf_P and FWEIGHT have thrust units.

- * Denotes a sampled quantity
- A Instantaneous acceleration
- A_A Actual acceleration (instantaneous acceleration at a specified sample instant). If no sample instant is specified, the current sample instant is implied.
- \tilde{A} Measured average acceleration during the preceding sample interval obtained by dividing the velocity increment measured over the preceding computation cycle by the elapsed time. (gravity ignored)
- A_C Extrapolated acceleration command. This command is based on the velocity error extrapolated to the time the current acceleration command increment is expected to be, in effect, achieved (i.e. the time an equivalent acceleration step is achieved as shown in Fig. A1 Appendix A).

δA_C	Acceleration command increment (extrapolated acceleration error).
δA_P	Acceleration correction increment which must be added to the measured average acceleration \tilde{A} to yield the actual acceleration A_A .
ACA	Attitude Control Assembly
DECA	Descent Engine Control Assembly. This is a digital-to-analog conversion device which couples the LGC to the descent engine. The input to the DECA is the LGC pulse train emitted at 3200 pulses (bits) per second, and the output is a throttle voltage. The output voltage corresponds to the cumulative count of input bits. The scaling is defined in Appendix C.
DELAY	The throttle routine's estimate of the time interval from the sample instant to the time the resulting equivalent acceleration step is commanded (Appendix A Fig. A1). This includes the computation delay plus half the actual time required to output the throttle pulses at 3200 pulses/second, and is, on the average, equal to LAG minus the estimated engine time constant THROTLAG.
ET	= $\exp(-T/TE)$
EA	= $\exp(-(T-D)/TE)$
GSOP	Guidance System Operations Plan (Ref. 4)
IMU	Inertial Measurement Unit
KFM	The actual sensitivity of the system to step changes in commanded acceleration divided by the sensitivity modeled by the guidance computer. This includes both the engine thrust sensitivity error and also the mass estimate error - hence the double tag FM. KFM = 1 means the system is correctly modeled by the guidance computer. KFM > 1 means the system provides a larger acceleration increment than expected.
LAG	The ROD guidance channel's estimate of the total time interval from the sample instant (the time the accelerometers are read) to the time the resulting equivalent acceleration step is achieved (Appendix A Fig. A1). This is the sum of the computation delay, the estimated engine time constant THROTLAG, and a nominal interval to account for half the average time required to output the throttle pulses at 3200 pulses/second.

LGC	LM Guidance Computer
LM	Lunar Module
LUMINARY	The LGC Program used during any manned lunar landing mission
MIT	Massachusetts Institute of Technology
NASA	National Aeronautics and Space Administration
ROD	Rate Of Descent guidance program
T	The sample time interval, i. e. 1 second
TAUENG	The actual time constant or time delay of the descent engine. It may be assumed that the engine responds either as a first order lag or as a pure delay.
TAUROD	The inverse of the gain of the ROD channel. If the sample interval were small with respect to TAUROD, the ROD guidance would null an altitude rate error exponentially with a time constant equal to TAUROD.
THROTLAG	The throttle routine's estimate of the engine time constant assuming the engine response is a first order lag.
V	Instantaneous velocity (altitude rate)
V_C	Commanded velocity (altitude rate)
δV	Velocity correction which must be added to the instantaneous velocity measured at the current sample instant to obtain the extrapolated velocity at the time the equivalent acceleration step is achieved. See Appendix A Fig. A1.

INTRODUCTION

A new terminal descent program featuring automatic nulling of the horizontal velocity components was designed and coded for Apollo 13 and subsequent missions. While testing the new program, Clinton Tillman of Grumman Aerospace Corporation noticed peculiar excursions of the descent engine throttle. These excursions occurred with a two second period (twice the sample period of the guidance program) and had a peak-to-peak amplitude of about 4 or 5% of the rated thrust of the descent engine. Because a time plot of these excursions had the appearance of a castellated nut, they became known as throttle castellations. Tillman searched the Apollo 11 and 12 telemetry data for similar phenomena, and discovered not only castellations similar to those in the new Apollo 13 program, but also throttle excursions of approximately 25% peak-to-peak relative to a center value of 27% of the rated thrust of the descent engine. Since the throttle excursions observed in the telemetry data were too large to be attributed to granularity and noise in the rate of descent algorithm, it was clear that another cause had to be found. Robert Covelli and Allan Klumpp of the MIT Draper Laboratory observed that the initiation of the oscillations seemed to be correlated with pitch attitude transients. The cause of this correlation was traced to the LM geometry shown in Fig. 1. Since the IMU is located substantially in front of the center of mass of the LM, these pitch rates produced IMU bobbing motions which were detected by the vertically sensing accelerometer. Because LM commander Conrad made only small pitch angle corrections about an erect attitude, the IMU bobbing motions produced were the same as if the IMU were replaced by the equivalent IMU shown in Fig. 1. Klumpp calculated that the IMU bobbing rates modulated the thrust and altitude rate estimates to an extent sufficient to cause the rate of descent (ROD) guidance program to command the initial erroneous throttle excursions.

Initial attempts to reproduce the pitch rates and the throttle excursions in bit-by-bit simulations (digital simulations of the LM descent including instruction-by-instruction simulation of the LM guidance computer (LGC)) were only partially successful. The pitch motions, including the precise timing coincidentally achieved by Conrad, were reproduced faithfully, and the onset of the oscillation occurred as expected, but the oscillation died out far faster in simulations than in flight. Consequently, at a meeting with NASA on the throttling problem, MIT reported that considerable modelling errors remained. James Alphin of the manned spacecraft center returned to the telemetry data in search of the modelling errors, and found

that the engine time constant was four to six times smaller than had been previously thought. When the correct engine time constant was used in the engine model, bit-by-bit simulation results were very similar to Apollo 12 telemetry data. Figure 2 shows the pitch rates produced by Conrad and reproduced by bit-by-bit simulation, and the resulting throttle and altitude rate responses. The vertical lines on Fig. 2 represent the instants at which the accelerometers were read in the ROD program. Note that the rate extremes (maximum or minimum and zero) coincide with the accelerometer readings, repetitively for 3 1/2 cycles (7 seconds), with phasing always such as to add energy to the system.

Utilizing the corrected engine model, a preliminary bit-by-bit simulation study was made to explore two approaches to reduce the throttle excursions. The first approach was to eliminate the excitation by correcting the accelerometer readings to refer the readings to the center of mass of the LM. The second approach was to enhance the stability of the system by adjusting the two throttle compensation constants dependent on the engine time constant, THROTLAG and LAG/TAU. The simulation results are illustrated by Figs. 3 and 4 which display progressively reduced throttle and altitude rate responses to pitch maneuvers. Figure 3, in which the accelerometer readings are not referred to the center of mass, shows that stabilizing the system by changing either THROTLAG or LAG/TAU substantially improves the system, and that changing both constants is apparently not much better than changing just one. Figure 4 shows that referring the accelerometer readings to the center of mass does more to reduce the amplitude of the throttle excursions than changing either of the throttle compensation constants, but does nothing to improve the system stability (i.e. the small oscillations which are produced die out no faster than they did in Fig. 3). The frames in the final column of Fig. 4 show the best empirically determined system.

The preliminary bit-by-bit simulation study demonstrated the need to refer the accelerometer readings to the center of mass and the need to modify the throttle compensation constants. However, due to the insensitivity of throttle behavior to small changes in the throttle compensation constants when the system poles are well within the stable region, the constants which yield the greatest stability margins would be difficult to determine with such an empirical study. That is, changes in system performance are noticeable only when the system approaches instability. Consequently, a Z transform analysis was used to determine the optimum throttle compensation constants and the corresponding stability margins. The remainder of this memo describes in detail the elimination of excitation with accelerometer reading corrections and the determination of throttle compensation constants with the Z transform analysis.

EXCITATION ELIMINATION

The primary source of throttle excitations observed in the Apollo 12 telemetry data was the coupling of pitch rate changes into the accelerometer measurements. Figure 1 illustrates the geometry associated with this excitation.

The concept for eliminating the excitation is to correct the accelerometer readings so that the accelerometers appear to be located at the center of mass. The complete vector equation for making this correction would be

$$\underline{\text{ACC}}_C = \underline{\text{ACC}}_U - \underline{\text{OMEGA}} \times (\underline{\text{RIMU}} - \underline{\text{RCM}})$$

where $\underline{\text{ACC}}_C$ is the corrected accelerometer reading vector, $\underline{\text{ACC}}_U$ is the uncorrected vector, $\underline{\text{OMEGA}}$ is the angular velocity vector of the spacecraft, $\underline{\text{RIMU}}$ is the position vector of the IMU, and $\underline{\text{RCM}}$ is the position vector of the center of mass. All vectors are expressed in IMU coordinates. Several simplifying assumptions can be made which reduce considerably the computations required.

These are:

1. The X IMU axis is vertical.
2. The spacecraft is essentially erect. This is necessarily true near touchdown; otherwise there would be a horizontal translational acceleration. Thus the X body axis is also vertical.
3. The center of mass is approximately on the X body axis.
4. The correction of horizontal acceleration measurements (Y and Z IMU axes) is unnecessary.
5. There is zero displacement between the center of mass and the IMU in the lateral (Y body) direction.

With these simplifying assumptions, the IMU could be replaced by the equivalent IMU shown in Fig. 1, and the correction reduces to the following scalar equation

$$\text{ACC}_{CX} = \text{ACC}_{UX} - \text{OMEGA}_Y \cdot \text{RIMU}_Z,$$

where ACC_{CX} and ACC_{UX} are the corrected and uncorrected X accelerometer readings and are still expressed in IMU coordinates, and OMEGA_Y and RIMU_Z are the pitch rate estimated by the digital autopilot and the IMU Z coordinate and are now expressed in body coordinates.

STABILITY ENHANCEMENT

A Z transform analysis was used to optimize the throttle compensation constants and determine the stability margins of the system. The sampled data model of the system used in the Z transform analysis is described below.

Model

Figure 5 is a linearized model of the ROD guidance channel. The following assumptions were used in deriving this model.

1. Because of linearity, the constant gravity bias can be ignored.
2. Velocities and accelerations are the inputs and outputs of the system and the conversions to thrust units within the system need not be represented.
3. Scaling errors, consisting of 1) thrust increment per bit throttle command and 2) mass error, can be treated by a single scaling constant KFM whose nominal value is unity.
4. All computation delays between the time the accelerometers are read (the sample time) and the time the throttle command is issued to the descent engine control assembly (DECA) can be modeled as a single pure delay at the computer-DECA interface.
5. The time duration required to output throttle increment bits to the DECA can be modeled by an equivalent delay of half the total duration. (See the derivation of the acceleration correction increment, Appendix A.) It can be shown that this assumption produces a plant model with slightly less gain than the actual plant. With this assumption, the delay D (shown in the block diagrams Figs. 5 thru 7) is a linear function of the acceleration command increment δA_C . D represents both the lumped computational delay and half the duration required to transmit the throttle increment bits. Because it is computed by the throttle program D appears both in the feed-forward path and in the feed-back path. D is assumed error free.

6. The engine response to a step change can be modeled as a first order lag as in the block diagrams and in the analysis, or as a pure time delay as in a portion of Appendix B.
7. The accelerometers are perfect and therefore need no compensation.
8. The thrust vector is always aligned with the local vertical.
9. Incorporation of landing radar measurements into the altitude rate estimate produces no change in the altitude rate estimate.

The block diagram of Fig. 5 was specially arranged to illuminate the essential design concepts of the ROD guidance. These design concepts are:

1. The system is designed to achieve a total acceleration proportional to the velocity error. Thus, for a continuous system approximation, or a sample interval short with respect to the inverse gain TV , the design concept is to reduce the velocity error exponentially with a time constant TV . The sampled data model is designed to have a single pole on the positive real axis located at $(TV - T)/TV$. Schindwolf (Ref. 1) and Appendix B show that when the engine is modeled as a pure delay and the compensation is exact, this simple result is achieved. The remaining concepts are the means for achieving this result.
2. The acceleration command increment (δA_C) issued by the throttle routine should drive the instantaneous acceleration (A) into coincidence with the extrapolated acceleration command (A_C) from the guidance program. The guidance program provides an estimate of the average acceleration (\tilde{A}) since the preceding sample instant based on the velocity increment measured during the preceding computation cycle. This average acceleration is not a good measure of the instantaneous acceleration because of the acceleration change made during the preceding sample period. Therefore, the throttle routine corrects the average acceleration by adding the acceleration correction increment (δA_P) to yield an estimate of the instantaneous acceleration at the current sample instant (the actual acceleration A_A). (See Appendix A for a derivation of the

acceleration correction increment.) The acceleration command increment is obtained by subtracting the actual acceleration from the extrapolated acceleration command.

3. The instantaneous acceleration should be time consistent with the instantaneous velocity error. Because a non-zero instantaneous acceleration will change the velocity error between the sample instant and the time the system responds, the ROD guidance algorithm extrapolates the velocity error to the time the acceleration command increment is expected to be, in effect, achieved (i.e. the time an equivalent acceleration step is achieved as shown in Appendix A Fig. A1). The extrapolated velocity error is the sample instant velocity error plus the actual acceleration multiplied by the total time lag. The total time lag consists of delay D due to the computation interval and half the time for issuing throttle bits plus the estimated engine time constant TT.

Figure 6 is identical to Fig. 5 except that boxes are combined and common factors are cancelled. Figure 7 is the Z transform representation of Fig. 6. The polynomial coefficients of the closed loop transfer function for the system illustrated in Fig. 7 are presented in Appendix B. In addition, Appendix B presents the polynomial coefficients obtained by modeling the engine as a pure time delay.

Parameter Settings

The following are the proposed throttle compensation constants for the ROD guidance channel, and the best estimate of the plant parameters.

PARAMETER	VALUE	COMPENSATION or PLANT
TAUROD	1.5 second	Comp
LAG	.35 second	Comp
(LAG/TAU)	(.233333)	Comp
THROTLAG	.08 second	Comp
TAUENG	.08 second	Plant
DELAY	.27 second	Plant
KFM	1.0	Plant

Note that with these gain settings the system compensation is consistent with the design concepts discussed in the preceding section, i.e. THROTLAG = TAUENG and LAG = DELAY + THROTLAG. Figure 8 shows the system roots and impulse response as determined by the sampled data model, and also the step response as determined by both the sampled data model and the bit-by-bit simulation. The marks on the time axis indicate one second sample instants. With these parameter settings the poles consist of a triplet essentially at the origin and a single pole on the positive real axis. The conditions for the bit-by-bit simulation are the same as for the minimally modified bit-by-bit simulation responses as described in Appendix C.

Stability Margins

Table 1 shows the stability regions determined with the Z transform analysis. Each of the six parameters is varied, keeping the remaining five at the nominal values. For each parameter, the columns of the table show the initial value considered, the last unstable value, the first stable value, the first unstable value, and the final value considered. If no change in the stability status was found, the column entry is X. Note that the stability regions for variations in plant parameters are far wider than any conceivable plant dispersions. That is, the system is stable for an engine time constant in excess of 0.9 second, for a computation delay in excess of 0.92 second, and for a thrust sensitivity to bit increments in excess of 2.3 times nominal. THROTLAG is the parameter with the smallest stability region (from -0.39 to +0.34 second).

Figures 9 thru 14, determined with the Z transform analysis, show the root loci and impulse and step responses versus each of the system parameters. On each figure, a single parameter is varied in forty equal steps from an initial value to a final value. The closed loop system poles are marked at each of these 41 cases numbered 000 to 040. If a case is of special interest, then the system zeros and the step and impulse responses are plotted, the first two step values and the pole and zero locations are listed above the plots, and the values of the parameters are listed below the plots. The special interest cases consist of 1) the initial and final values and every eighth case between, 2) the case in which the parameter being varied is closest to its nominal value, 3) each stable case

in which the preceding case is unstable (identified above the plots with a single asterisk), and 4) each unstable case in which the preceding case was stable (identified above the plots with a double asterisk). Thus the stable region is between the single and double asterisks.

Figure 15 thru 26 display the system behavior at each extreme parameter value. The extreme value is the first or last stable value if a stability limit exists. Otherwise the extreme value is limited by ability to simulate (e.g. numerical integration considerations require the engine time constant to be no less than about .05 second) or by reasonableness (e.g. we felt that TAUROD in excess of 2.00 need not be considered). These figures show the root locations and the impulse response as determined by the sampled data analysis. They also show step responses from three sources, 1) sampled data analysis - solid line, 2) bit-by-bit simulations with the minimum number of modifications required to simulate the extreme cases - dashed line, 3) bit-by-bit simulations modified as necessary to adhere as closely as possible to the conditions of the Z transform analysis - dotted line. The conditions for the bit-by-bit simulations are described in Appendix C.

CONCLUSIONS

Two measures have been taken to correct the ROD guidance: 1) the accelerometer readings have been corrected to refer the readings to the center of mass, and 2) the system has been properly compensated according to the original design philosophy. Referring the accelerometer readings to the center of mass almost completely eliminates excitation of the ROD guidance by pitch rates. Correctly setting the throttle compensation constants produces a system in which the stability margins are far wider than conceivable variations in the plant parameters.

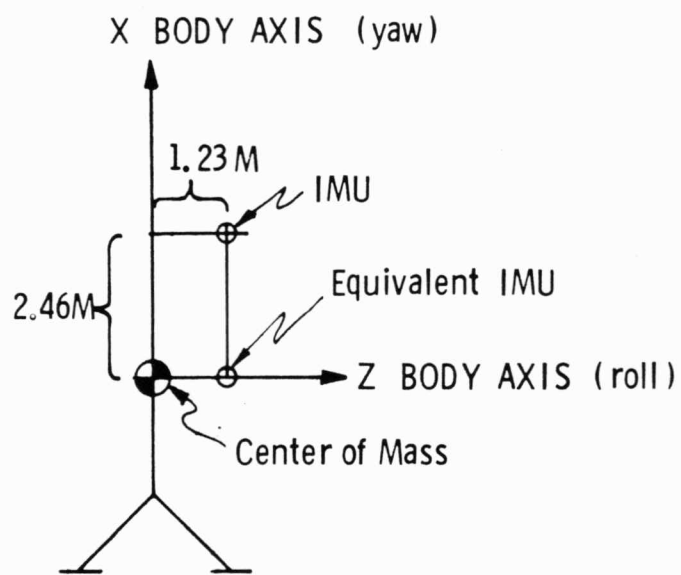
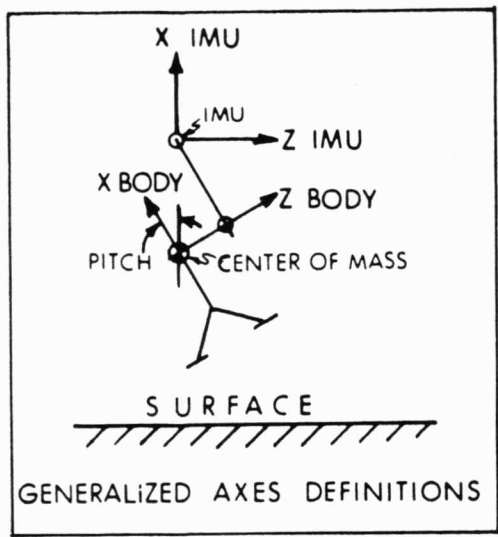
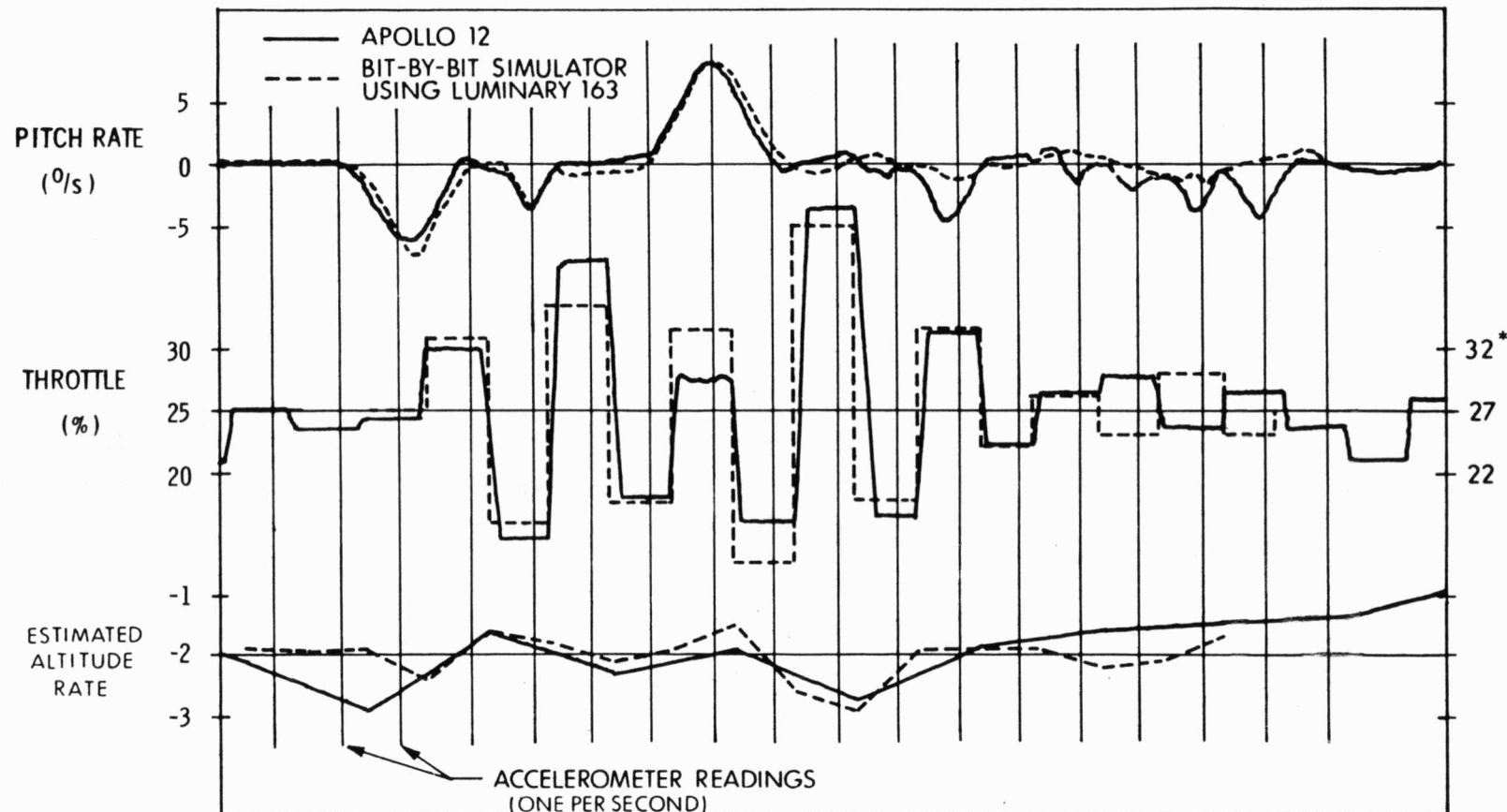


Fig. 1 LM Geometry Responsible for Exciting the ROD Guidance with Pitch Rates



*THIS SCALE FOR bit-by-bit.
2% DIFFERENCE DUE TO SLIGHTLY
DIFFERENT MASS AND THROTTLE
CALIBRATION.

Fig. 2 Apollo 12 and Bit-by-bit Simulator Response to Pitch Rates

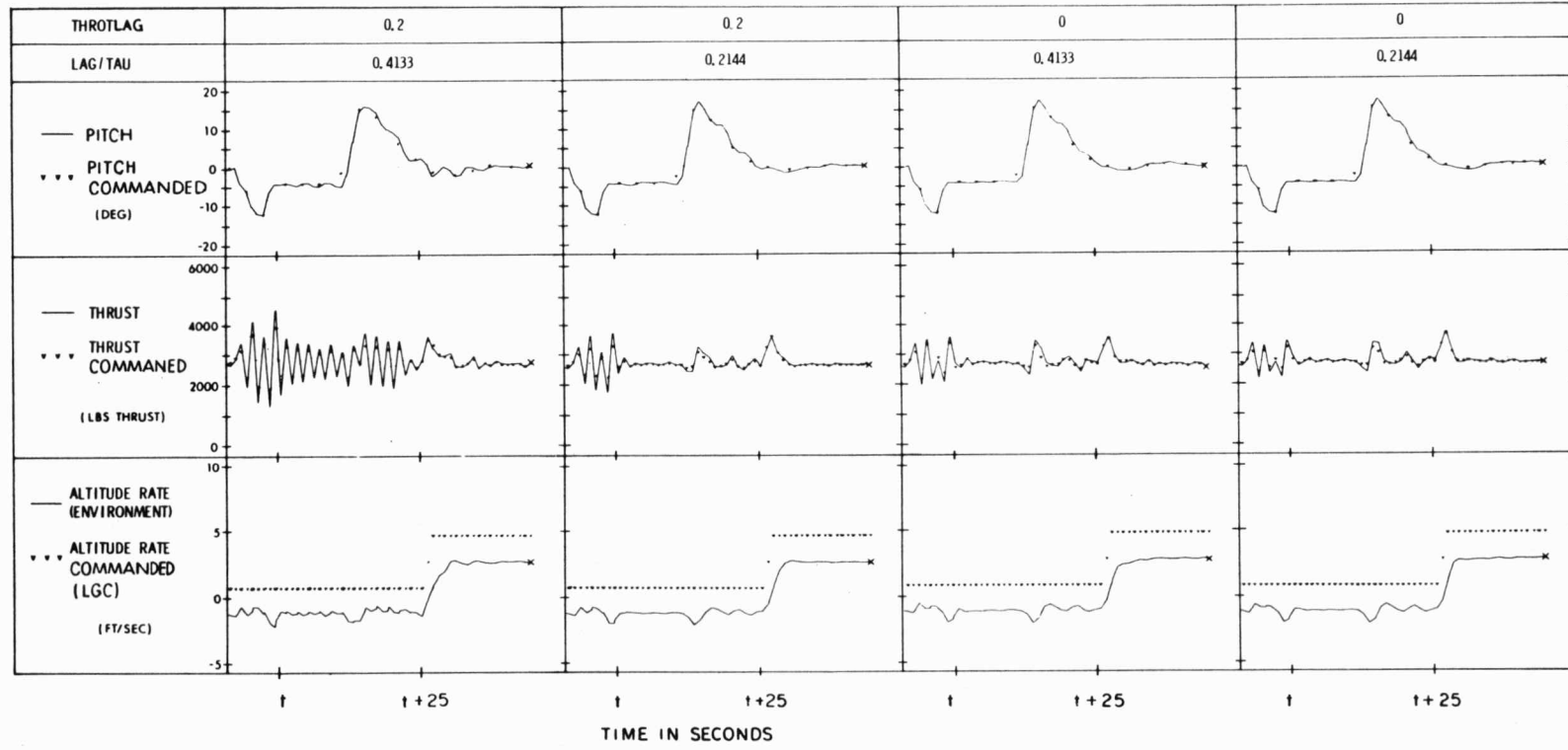


Fig. 3 Response to Attitude and Altitude Rate Inputs for Various ROD Parameters with Accelerometer Readings not Referred to the Center of Mass

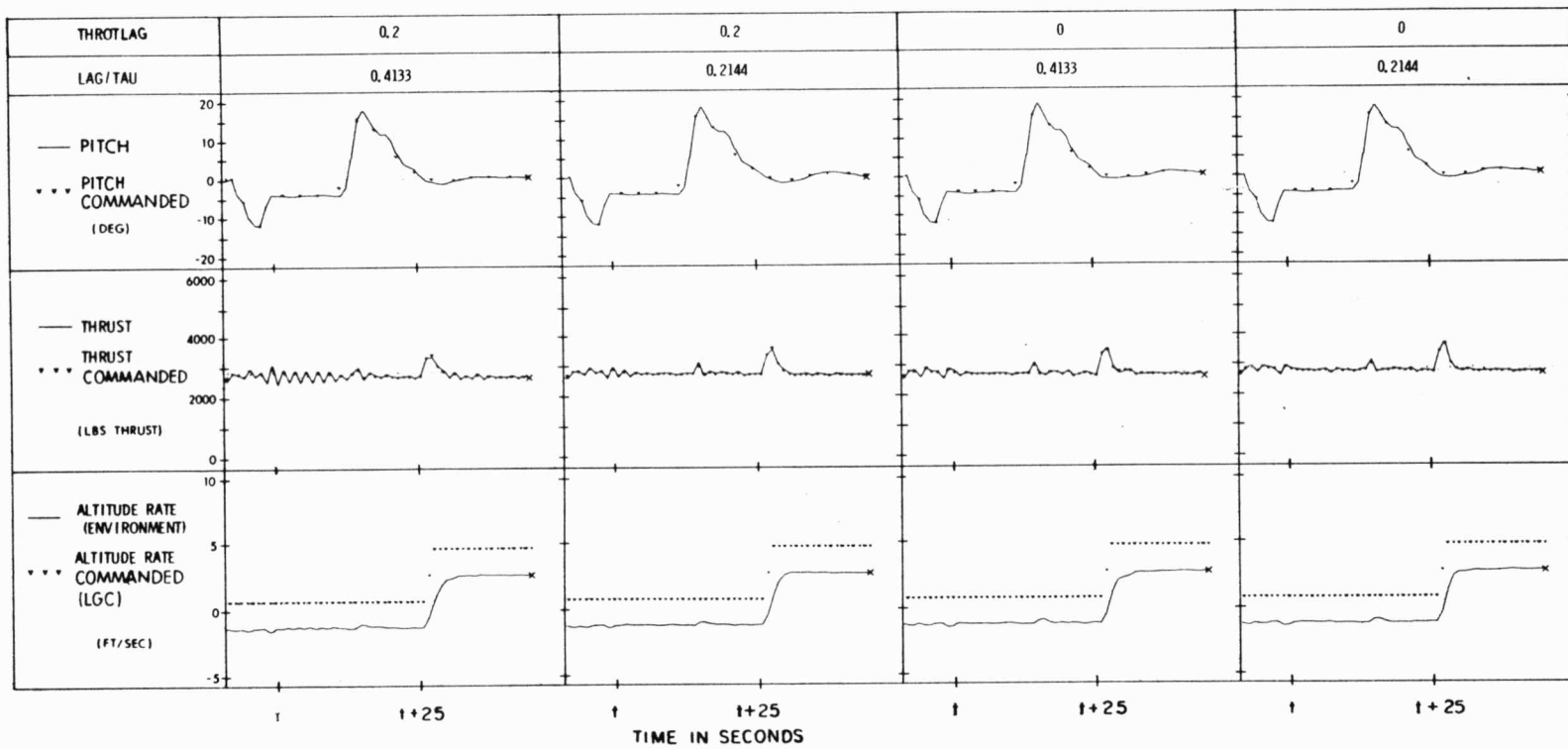


Fig. 4 Response to Attitude and Altitude Rate Inputs for Various ROD Parameters with Accelerometer Readings Referred to the Center of Mass

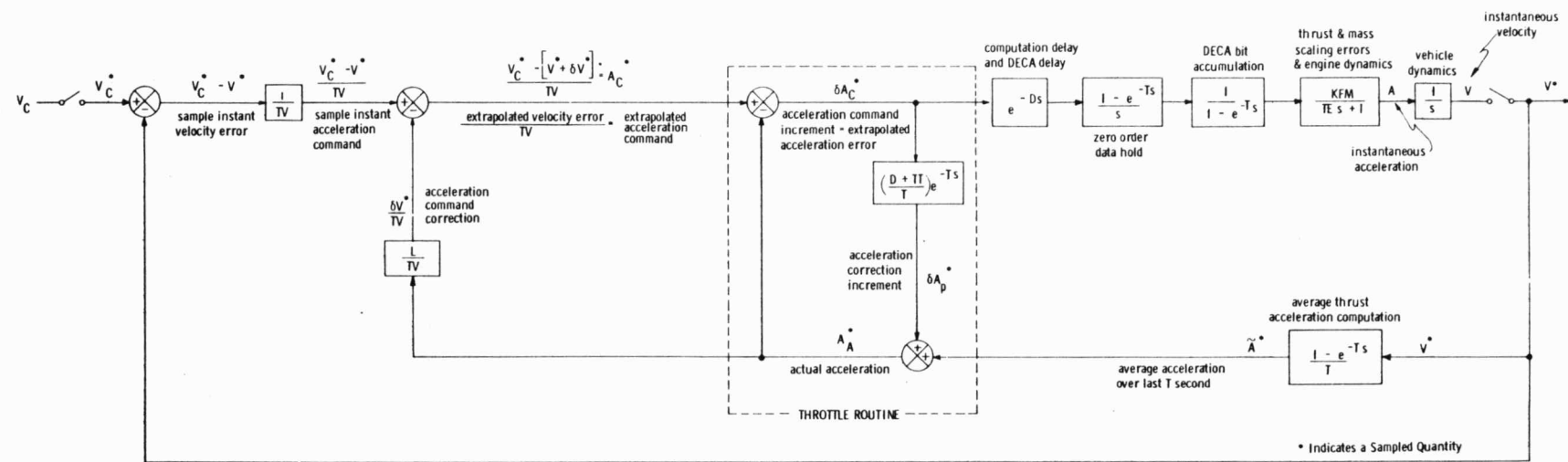


Fig. 5 ROD Guidance Channel Linearized Block Diagram

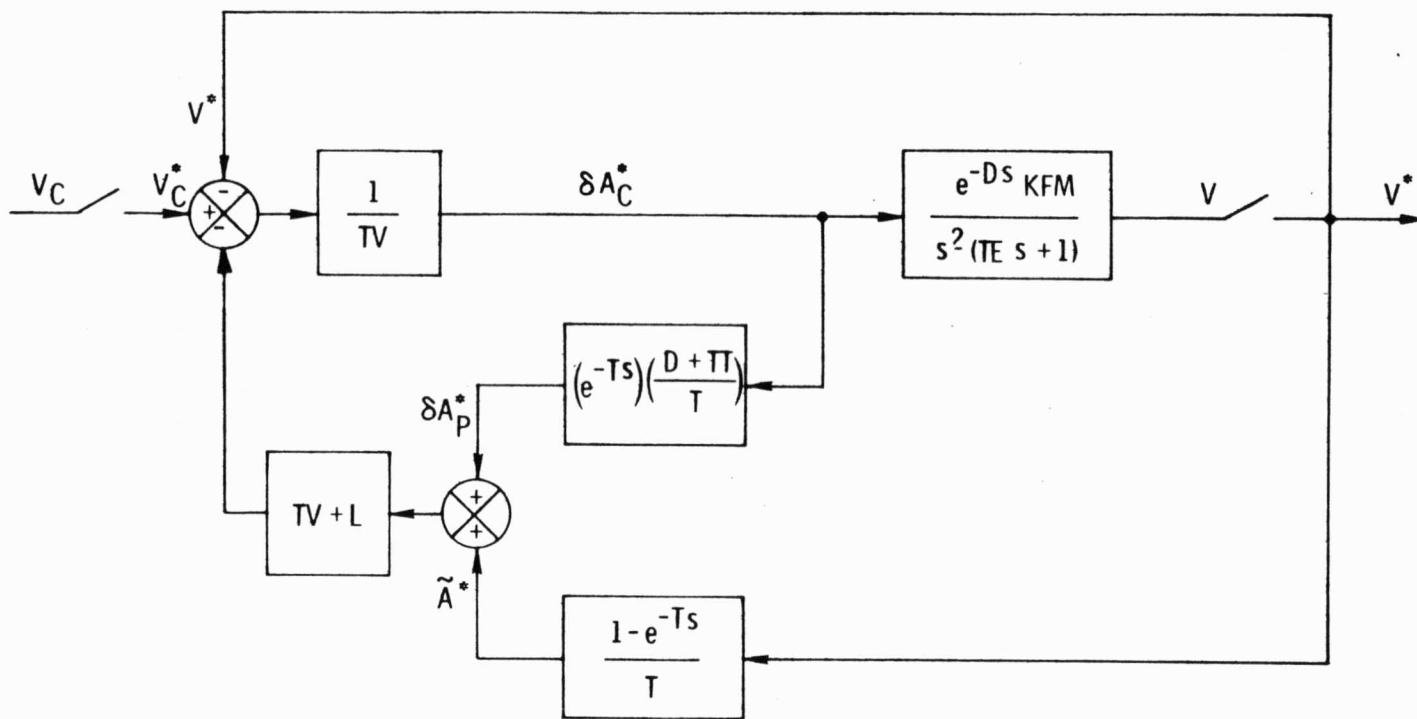


Fig. 6 ROD Guidance Channel Reduced Linearized Block Diagram

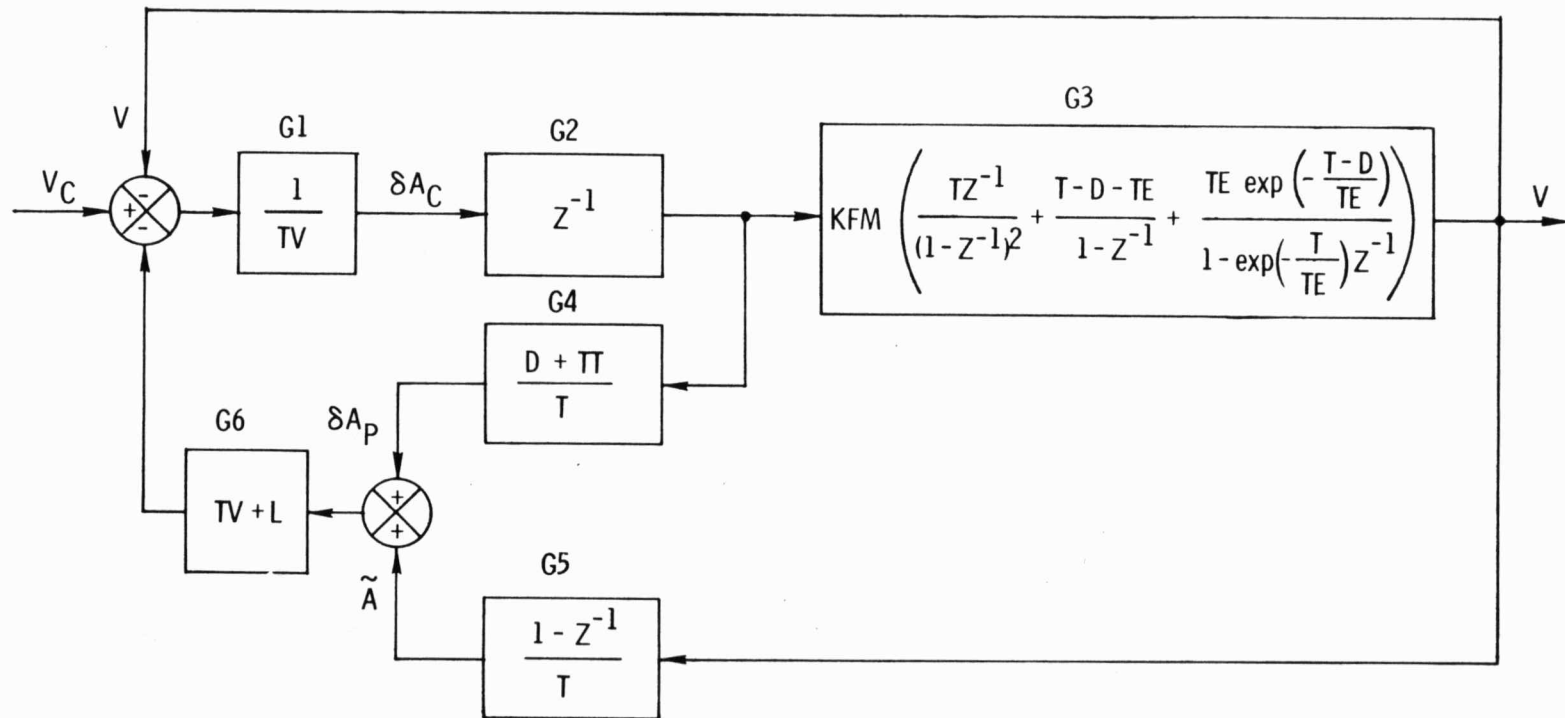


Fig. 7 ROD Guidance Channel Reduced Z Transform Diagram

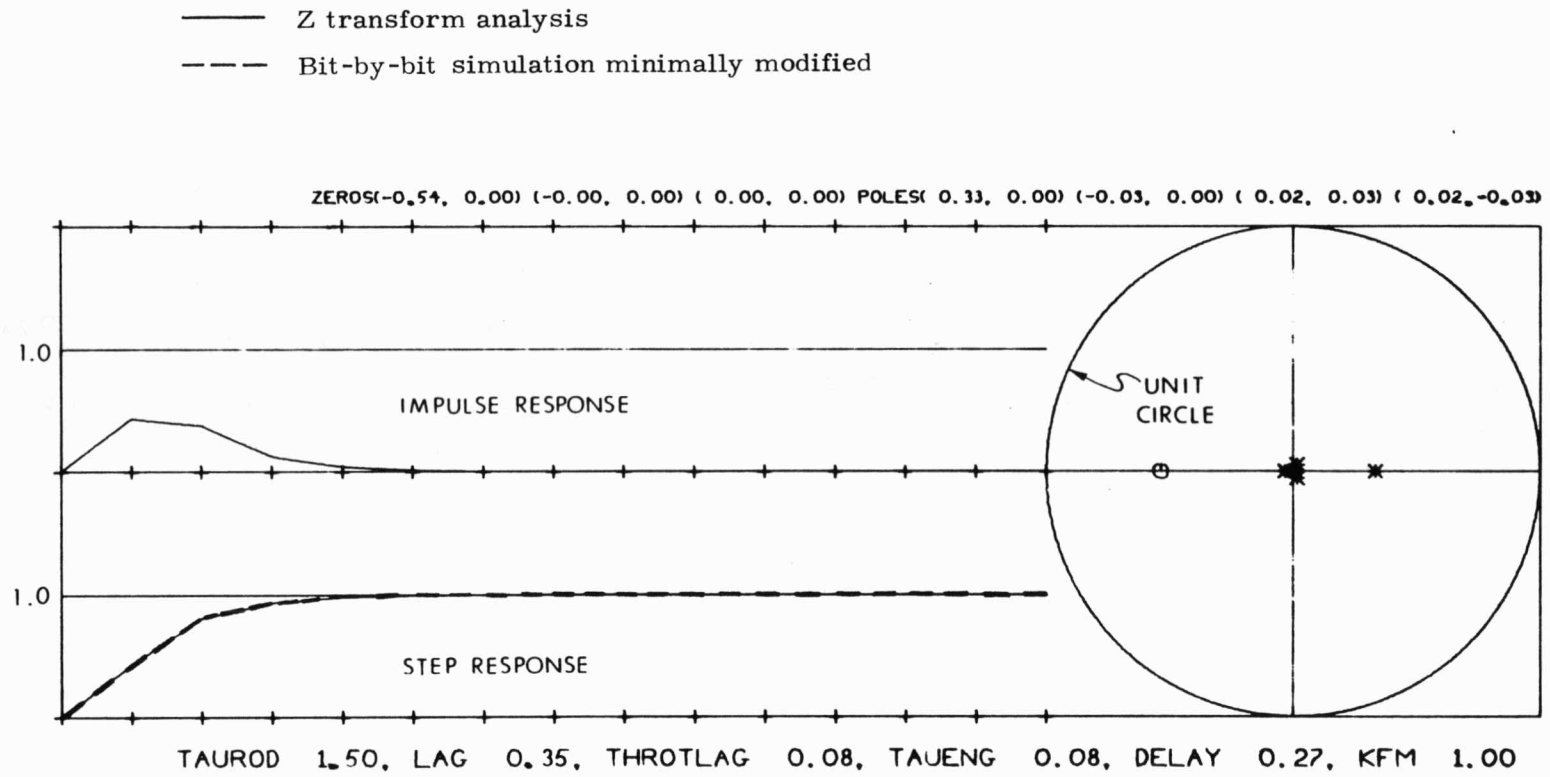
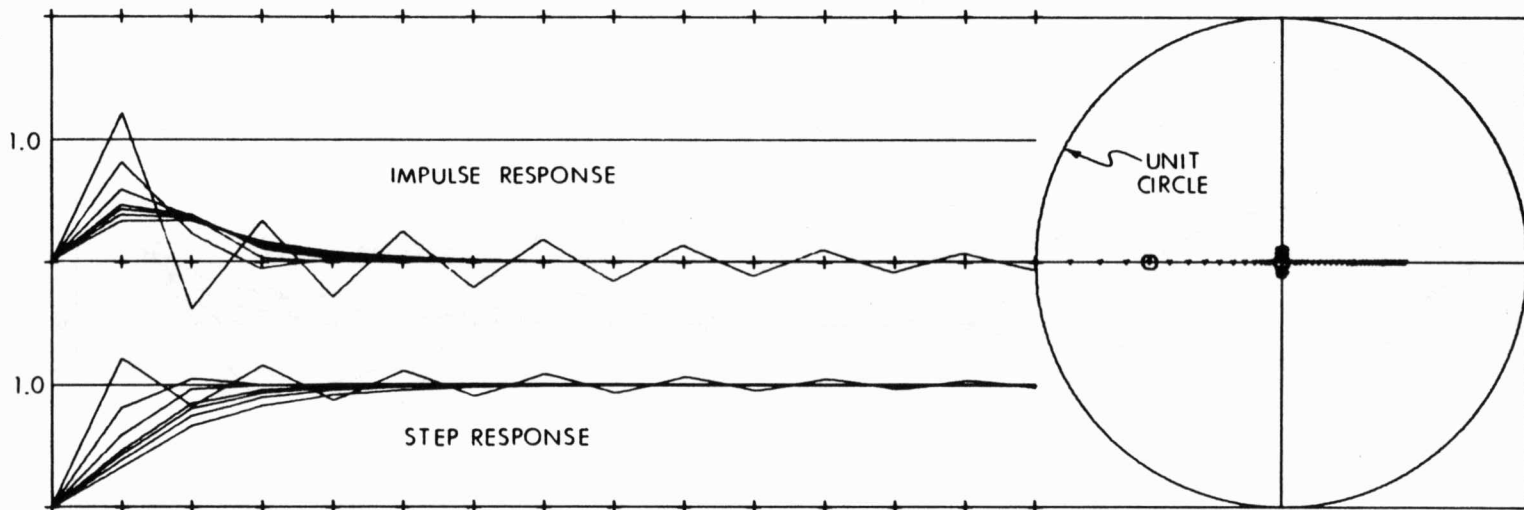


Fig. 8 Performance and roots for proposed Apollo 14 ROD parameters.

	INITIAL VALUE	LAST UNSTABLE VALUE	FIRST STABLE VALUE	LAST STABLE VALUE	FIRST UNSTABLE VALUE	FINAL VALUE
TAUROD	.5	.5	.5375	X	X	2.0
LAG	-1.2	-1.2	-1.136	1.306	1.37	1.37
THROTLAG	-.41	-.41	-.391	.341	.36	.36
TAUENG	0	X	X	.907	.93	.93
DELAY	0	X	X	X	X	.92
KFM	.1	X	X	2.342	2.4	2.4

Table 1 STABILITY REGIONS FOR EACH PARAMETER DETERMINED WITH Z TRANSFORM ANALYSIS

CASE
 040 STEP(0.32, 0.66) ZEROS(-0.54, 0.00) (-0.00, 0.00) (0.00, 0.00) POLES(0.50, 0.00) (-0.03, 0.00) (0.01, 0.02) (0.01,-0.02)
 032 STEP(0.38, 0.75) ZEROS(-0.54, 0.00) (-0.00, 0.00) (0.00, 0.00) POLES(0.41, 0.00) (-0.03, 0.00) (0.01, 0.03) (0.01,-0.03)
 027 STEP(0.43, 0.81) ZEROS(-0.54, 0.00) (-0.00, 0.00) (0.00, 0.00) POLES(0.34, 0.00) (-0.03, 0.00) (0.02, 0.03) (0.02,-0.03)
 024 STEP(0.46, 0.85) ZEROS(-0.54, 0.00) (-0.00, 0.00) (0.00, 0.00) POLES(0.29, 0.00) (-0.03, 0.00) (0.02, 0.03) (0.02,-0.03)
 016 STEP(0.59, 0.96) ZEROS(-0.54, 0.00) (-0.00, 0.00) (0.00, 0.00) POLES(0.10, 0.00) (0.02, 0.05) (0.02,-0.05) (-0.05, 0.00)
 008 STEP(0.81, 1.05) ZEROS(-0.54, 0.00) (-0.00, 0.00) (0.00, 0.00) POLES(-0.25, 0.00) (-0.02, 0.03) (-0.02,-0.03) (0.03, 0.00)
 * 001 STEP(1.21, 0.82) ZEROS(-0.54, 0.00) (-0.00, 0.00) (0.00, 0.00) POLES(-0.86, 0.00) (-0.01, 0.02) (-0.01,-0.02) (0.02, 0.00) *
 000 STEP(1.30, 0.70) ZEROS(-0.54, 0.00) (-0.00, 0.00) (0.00, 0.00) POLES(-1.00, 0.00) (-0.01, 0.02) (-0.01,-0.02) (0.02, 0.00)



000	TAUROD	0.50,	LAG	0.35,	THROTLAG	0.08,	TAUENG	0.08,	DELAY	0.27,	KFM	1.00
001	TAUROD	0.54,	LAG	0.35,	THROTLAG	0.08,	TAUENG	0.08,	DELAY	0.27,	KFM	1.00
008	TAUROD	0.80,	LAG	0.35,	THROTLAG	0.08,	TAUENG	0.08,	DELAY	0.27,	KFM	1.00
016	TAUROD	1.10,	LAG	0.35,	THROTLAG	0.08,	TAUENG	0.08,	DELAY	0.27,	KFM	1.00
024	TAUROD	1.40,	LAG	0.35,	THROTLAG	0.08,	TAUENG	0.08,	DELAY	0.27,	KFM	1.00
027	TAUROD	1.51,	LAG	0.35,	THROTLAG	0.08,	TAUENG	0.08,	DELAY	0.27,	KFM	1.00
032	TAUROD	1.70,	LAG	0.35,	THROTLAG	0.08,	TAUENG	0.08,	DELAY	0.27,	KFM	1.00
040	TAUROD	2.00,	LAG	0.35,	THROTLAG	0.08,	TAUENG	0.08,	DELAY	0.27,	KFM	1.00

CASE

Fig. 9 Performance and roots vs TAUROD.

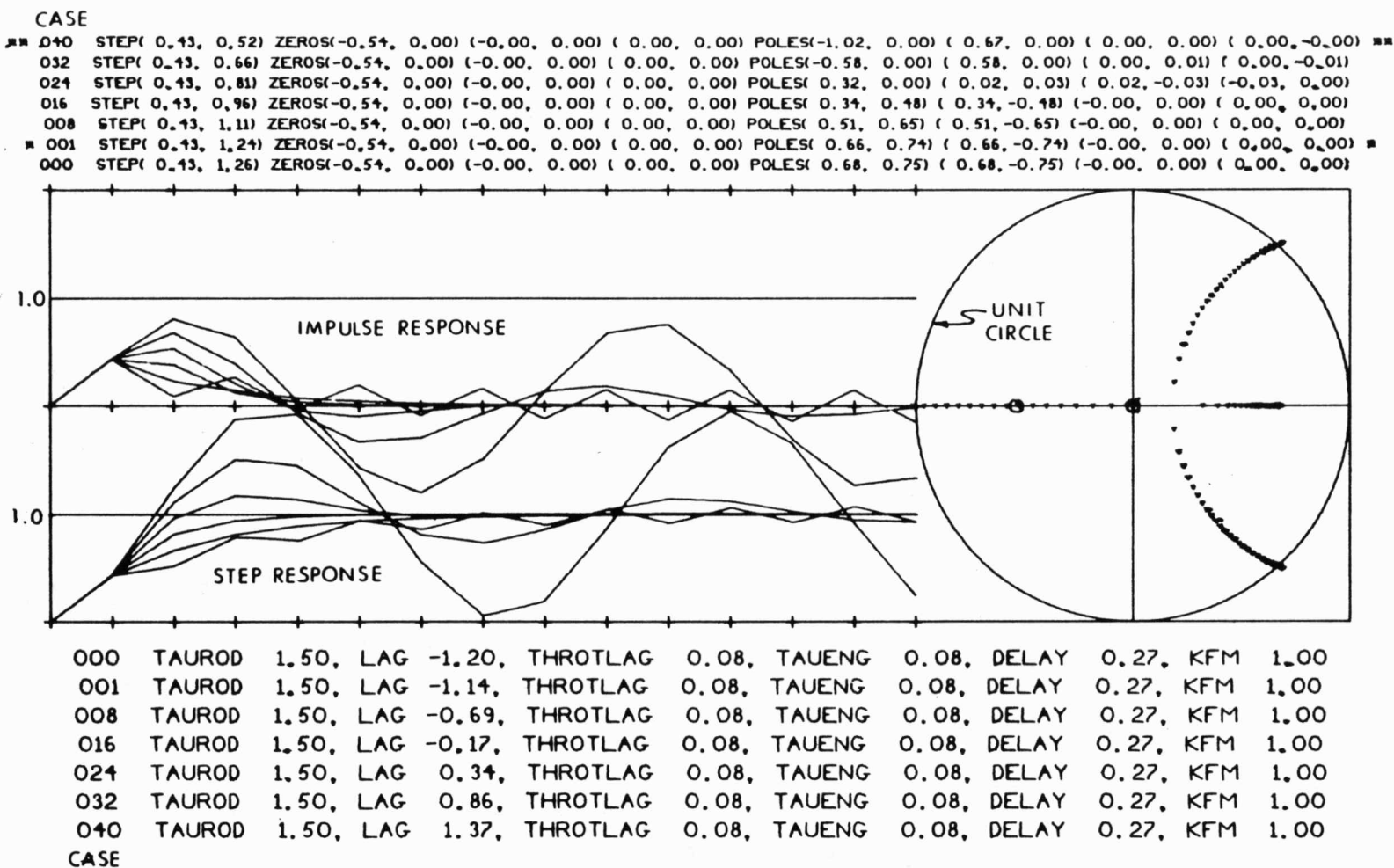
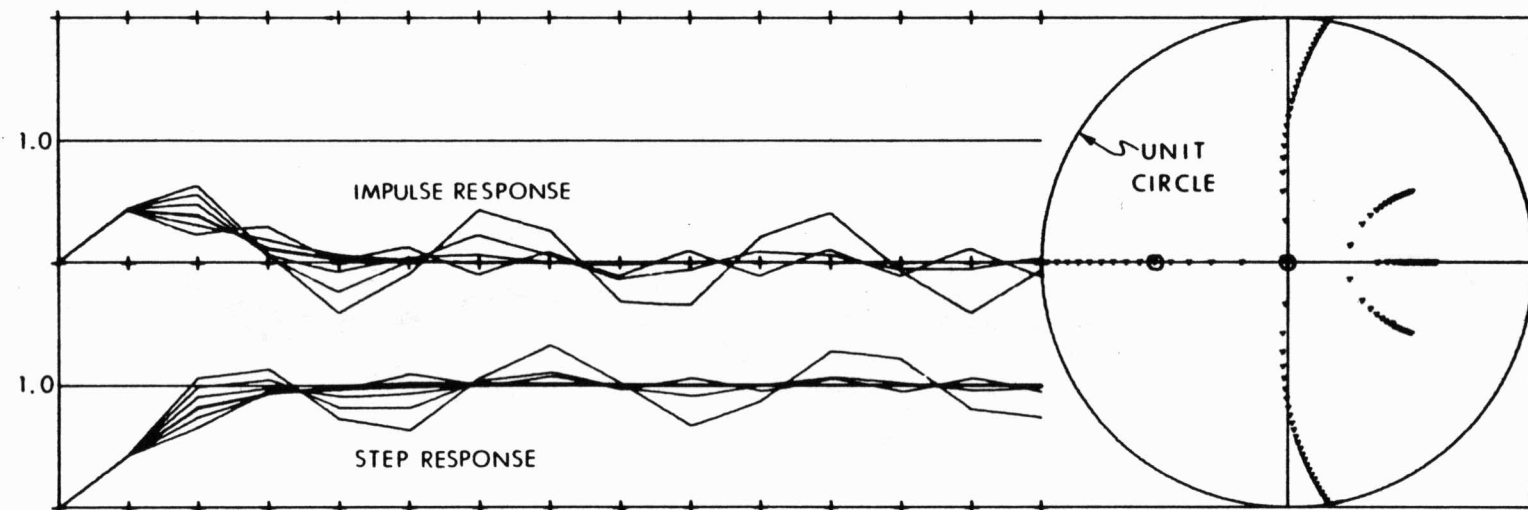


Fig. 10 Performance and roots vs LAG.

CASE
 ■■ 040 STEP(0.43, 0.66) ZEROS(-0.54, 0.00) (-0.00, 0.00) (0.00, 0.00) POLES(-1.02, 0.00) (0.50, 0.29) (0.50,-0.29) (0.00, 0.00) ■■
 032 STEP(0.43, 0.74) ZEROS(-0.54, 0.00) (-0.00, 0.00) (0.00, 0.00) POLES(-0.66, 0.00) (0.12, 0.25) (0.12,-0.25) (0.00, 0.00)
 025 STEP(0.43, 0.82) ZEROS(-0.54, 0.00) (-0.00, 0.00) (0.00, 0.00) POLES(0.37, 0.00) (-0.01, 0.17) (-0.01,-0.17) (-0.00, 0.00)
 024 STEP(0.43, 0.83) ZEROS(-0.54, 0.00) (-0.00, 0.00) (0.00, 0.00) POLES(0.41, 0.00) (-0.02, 0.29) (-0.02,-0.29) (-0.00, 0.00)
 016 STEP(0.43, 0.91) ZEROS(-0.54, 0.00) (-0.00, 0.00) (0.00, 0.00) POLES(0.02, 0.66) (0.02,-0.66) (0.52, 0.00) (-0.00, 0.00)
 008 STEP(0.43, 0.99) ZEROS(-0.54, 0.00) (-0.00, 0.00) (0.00, 0.00) POLES(0.09, 0.85) (0.09,-0.85) (0.57, 0.00) (-0.00, 0.00)
 ■ 001 STEP(0.43, 1.06) ZEROS(-0.54, 0.00) (-0.00, 0.00) (0.00, 0.00) POLES(0.16, 0.97) (0.16,-0.97) (0.60, 0.00) (-0.00, 0.00) ■■
 000 STEP(0.43, 1.07) ZEROS(-0.54, 0.00) (-0.00, 0.00) (0.00, 0.00) POLES(0.17, 0.99) (0.17,-0.99) (0.60, 0.00) (-0.00, 0.00)



000	TAUROD	1.50,	LAG	0.35,	THROTLAG	-0.41,	TAUENG	0.08,	DELAY	0.27,	KFM	1.00
001	TAUROD	1.50,	LAG	0.35,	THROTLAG	-0.39,	TAUENG	0.08,	DELAY	0.27,	KFM	1.00
008	TAUROD	1.50,	LAG	0.35,	THROTLAG	-0.26,	TAUENG	0.08,	DELAY	0.27,	KFM	1.00
016	TAUROD	1.50,	LAG	0.35,	THROTLAG	-0.10,	TAUENG	0.08,	DELAY	0.27,	KFM	1.00
024	TAUROD	1.50,	LAG	0.35,	THROTLAG	0.05,	TAUENG	0.08,	DELAY	0.27,	KFM	1.00
025	TAUROD	1.50,	LAG	0.35,	THROTLAG	0.07,	TAUENG	0.08,	DELAY	0.27,	KFM	1.00
032	TAUROD	1.50,	LAG	0.35,	THROTLAG	0.21,	TAUENG	0.08,	DELAY	0.27,	KFM	1.00
040	TAUROD	1.50,	LAG	0.35,	THROTLAG	0.36,	TAUENG	0.08,	DELAY	0.27,	KFM	1.00

CASE

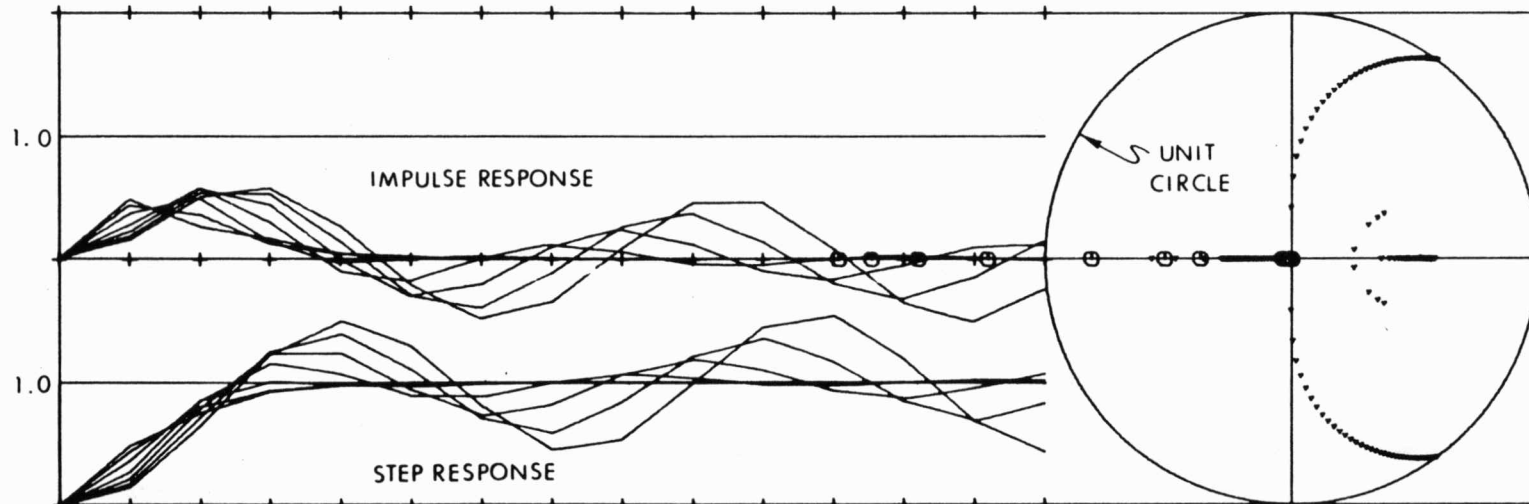
Fig. 11 Performance and roots vs THROTLAG.

CASE

```

** 040 STEP( 0.15, 0.65) ZEROS(-1.84, 0.00) (-0.04, 0.00) ( 0.00, 0.00) POLES( 0.59, 0.81) ( 0.59,-0.81) ( 0.58, 0.00) (-0.28, 0.00) **
032 STEP( 0.18, 0.72) ZEROS(-1.70, 0.00) (-0.03, 0.00) ( 0.00, 0.00) POLES( 0.51, 0.81) ( 0.51,-0.81) ( 0.56, 0.00) (-0.25, 0.00)
024 STEP( 0.22, 0.79) ZEROS(-1.52, 0.00) (-0.03, 0.00) ( 0.00, 0.00) POLES( 0.39, 0.80) ( 0.39,-0.80) ( 0.54, 0.00) (-0.20, 0.00)
016 STEP( 0.27, 0.85) ZEROS(-1.23, 0.00) (-0.02, 0.00) ( 0.00, 0.00) POLES( 0.24, 0.74) ( 0.24,-0.74) ( 0.51, 0.00) (-0.13, 0.00)
008 STEP( 0.37, 0.86) ZEROS(-0.81, 0.00) (-0.00, 0.00) ( 0.00, 0.00) POLES( 0.06, 0.53) ( 0.06,-0.53) ( 0.45, 0.00) (-0.03, 0.00)
003 STEP( 0.44, 0.80) ZEROS(-0.51, 0.00) (-0.00, 0.00) ( 0.00, 0.00) POLES( 0.25, 0.04) ( 0.25,-0.04) (-0.19, 0.00) ( 0.00, 0.00)
000 STEP( 0.49, 0.75) ZEROS(-0.37, 0.00) ( 0.00, 0.00) ( 0.00, 0.00) POLES(-0.57, 0.00) ( 0.37, 0.18) ( 0.37,-0.18) ( 0.00, 0.00)

```



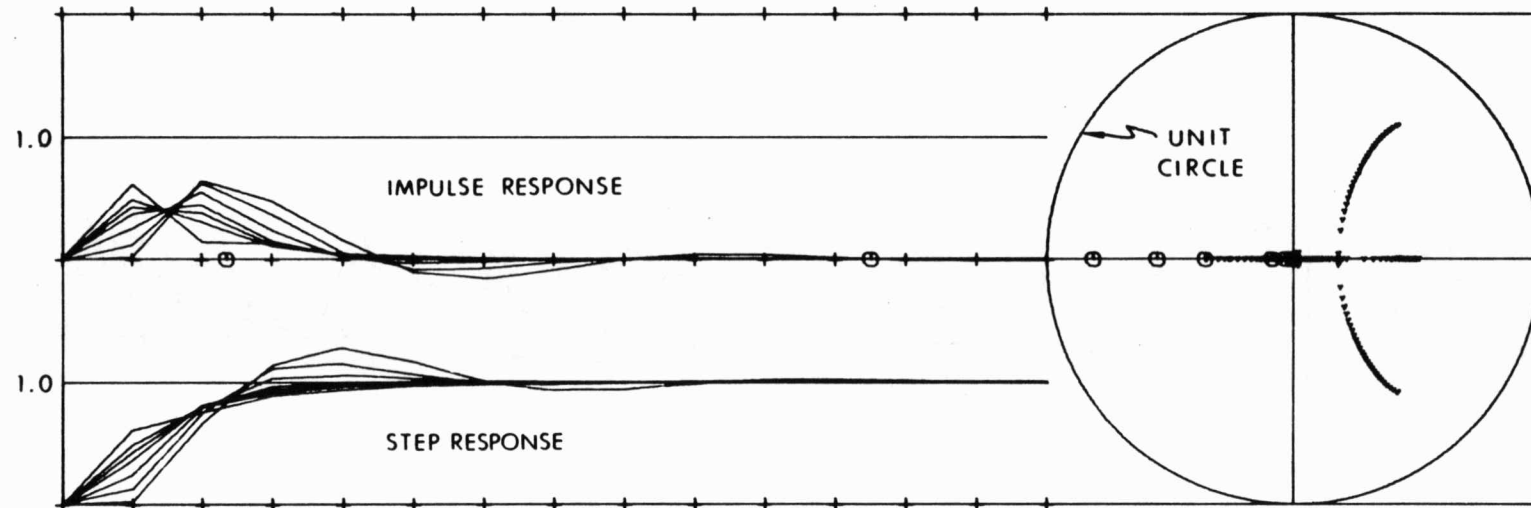
000	TAUROD	1.50,	LAG	0.35,	THROTLAG	0.08,	TAUENG	0.00,	DELAY	0.27,	KFM	1.00
003	TAUROD	1.50,	LAG	0.35,	THROTLAG	0.08,	TAUENG	0.07,	DELAY	0.27,	KFM	1.00
008	TAUROD	1.50,	LAG	0.35,	THROTLAG	0.08,	TAUENG	0.19,	DELAY	0.27,	KFM	1.00
016	TAUROD	1.50,	LAG	0.35,	THROTLAG	0.08,	TAUENG	0.37,	DELAY	0.27,	KFM	1.00
024	TAUROD	1.50,	LAG	0.35,	THROTLAG	0.08,	TAUENG	0.56,	DELAY	0.27,	KFM	1.00
032	TAUROD	1.50,	LAG	0.35,	THROTLAG	0.08,	TAUENG	0.74,	DELAY	0.27,	KFM	1.00
040	TAUROD	1.50,	LAG	0.35,	THROTLAG	0.08,	TAUENG	0.93,	DELAY	0.27,	KFM	1.00

CASE

Fig. 12 Performance and roots vs TAUENG.

CASE

040 STEP(0.02, 0.66) ZEROS(81.11, 0.00) (-0.03, 0.00) (0.00, 0.00) POLES(0.42, 0.54) (0.42, -0.54) (-0.35, 0.00) (0.22, 0.00)
 032 STEP(0.12, 0.74) ZEROS(-4.33, 0.00) (-0.00, 0.00) (0.00, 0.00) POLES(0.33, 0.16) (0.33, -0.16) (-0.12, 0.00) (0.10, 0.00)
 024 STEP(0.25, 0.79) ZEROS(-1.71, 0.00) (-0.00, 0.00) (0.00, 0.00) POLES(0.26, 0.35) (0.26, -0.35) (-0.04, 0.00) (0.04, 0.00)
 016 STEP(0.37, 0.81) ZEROS(-0.81, 0.00) (-0.00, 0.00) (0.00, 0.00) POLES(0.20, 0.16) (0.20, -0.16) (0.02, 0.00) (-0.02, 0.00)
 012 STEP(0.43, 0.81) ZEROS(-0.55, 0.00) (-0.00, 0.00) (0.00, 0.00) POLES(0.33, 0.00) (0.02, 0.03) (0.02, -0.03) (-0.03, 0.00)
 008 STEP(0.49, 0.80) ZEROS(-0.36, 0.00) (-0.00, 0.00) (0.00, 0.00) POLES(0.41, 0.00) (-0.14, 0.00) (0.00, 0.01) (0.00, -0.01)
 000 STEP(0.61, 0.76) ZEROS(-0.09, 0.00) (0.00, 0.00) (0.00, 0.00) POLES(0.51, 0.00) (-0.35, 0.00) (0.00, 0.00) (0.00, -0.00)



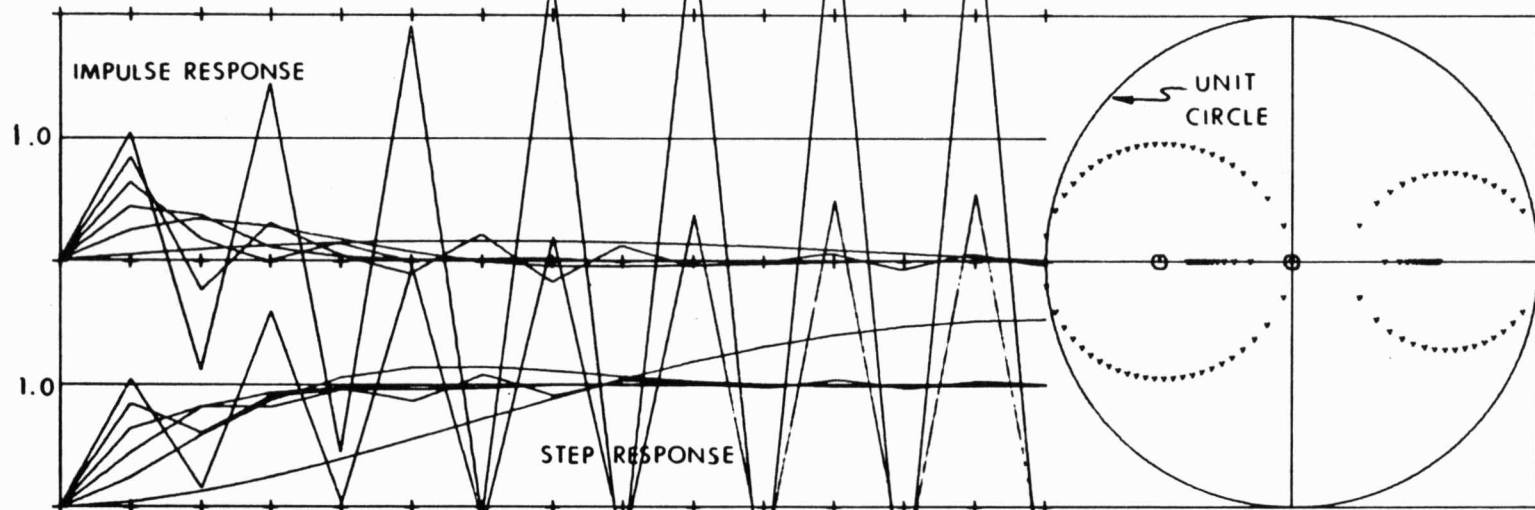
000	TAUROD	1.50,	LAG	0.35,	THROTLAG	0.08,	TAUENG	0.08,	DELAY	0.00,	KFM	1.00
008	TAUROD	1.50,	LAG	0.35,	THROTLAG	0.08,	TAUENG	0.08,	DELAY	0.18,	KFM	1.00
012	TAUROD	1.50,	LAG	0.35,	THROTLAG	0.08,	TAUENG	0.08,	DELAY	0.28,	KFM	1.00
016	TAUROD	1.50,	LAG	0.35,	THROTLAG	0.08,	TAUENG	0.08,	DELAY	0.37,	KFM	1.00
024	TAUROD	1.50,	LAG	0.35,	THROTLAG	0.08,	TAUENG	0.08,	DELAY	0.55,	KFM	1.00
032	TAUROD	1.50,	LAG	0.35,	THROTLAG	0.08,	TAUENG	0.08,	DELAY	0.74,	KFM	1.00
040	TAUROD	1.50,	LAG	0.35,	THROTLAG	0.08,	TAUENG	0.08,	DELAY	0.92,	KFM	1.00

CASE

Fig. 13 Performance and roots vs DELAY.

CASE

```
■■ 040 STEP( 1.04, 0.15) ZEROS(-0.54, 0.00) (-0.00, 0.00) ( 0.00, 0.00) POLES(-1.00, 0.10) (-1.00,-0.10) ( 0.60, 0.00) (-0.00, 0.00) ■■
032 STEP( 0.84, 0.60) ZEROS(-0.54, 0.00) (-0.00, 0.00) ( 0.00, 0.00) POLES(-0.71, 0.14) (-0.71,-0.14) ( 0.58, 0.00) (-0.00, 0.00)
024 STEP( 0.64, 0.82) ZEROS(-0.54, 0.00) (-0.00, 0.00) ( 0.00, 0.00) POLES(-0.40, 0.16) (-0.40,-0.16) ( 0.55, 0.00) (-0.00, 0.00)
016 STEP( 0.44, 0.82) ZEROS(-0.54, 0.00) (-0.00, 0.00) ( 0.00, 0.00) POLES( 0.34, 0.00) (-0.03, 0.15) (-0.03,-0.15) (-0.00, 0.00)
008 STEP( 0.24, 0.59) ZEROS(-0.54, 0.00) (-0.00, 0.00) ( 0.00, 0.00) POLES( 0.62, 0.36) ( 0.62,-0.36) (-0.37, 0.00) ( 0.00, 0.00)
000 STEP( 0.04, 0.13) ZEROS(-0.54, 0.00) (-0.00, 0.00) ( 0.00, 0.00) POLES( 0.93, 0.21) ( 0.93,-0.21) (-0.42, 0.00) ( 0.00, 0.00)
```



000	TAUROD	1.50,	LAG	0.35,	THROTLAG	0.08,	TAUENG	0.08,	DELAY	0.27,	KFM	0.10
008	TAUROD	1.50,	LAG	0.35,	THROTLAG	0.08,	TAUENG	0.08,	DELAY	0.27,	KFM	0.56
016	TAUROD	1.50,	LAG	0.35,	THROTLAG	0.08,	TAUENG	0.08,	DELAY	0.27,	KFM	1.02
024	TAUROD	1.50,	LAG	0.35,	THROTLAG	0.08,	TAUENG	0.08,	DELAY	0.27,	KFM	1.48
032	TAUROD	1.50,	LAG	0.35,	THROTLAG	0.08,	TAUENG	0.08,	DELAY	0.27,	KFM	1.94
040	TAUROD	1.50,	LAG	0.35,	THROTLAG	0.08,	TAUENG	0.08,	DELAY	0.27,	KFM	2.40

CASE

Fig. 14 Performance and roots vs KFM.

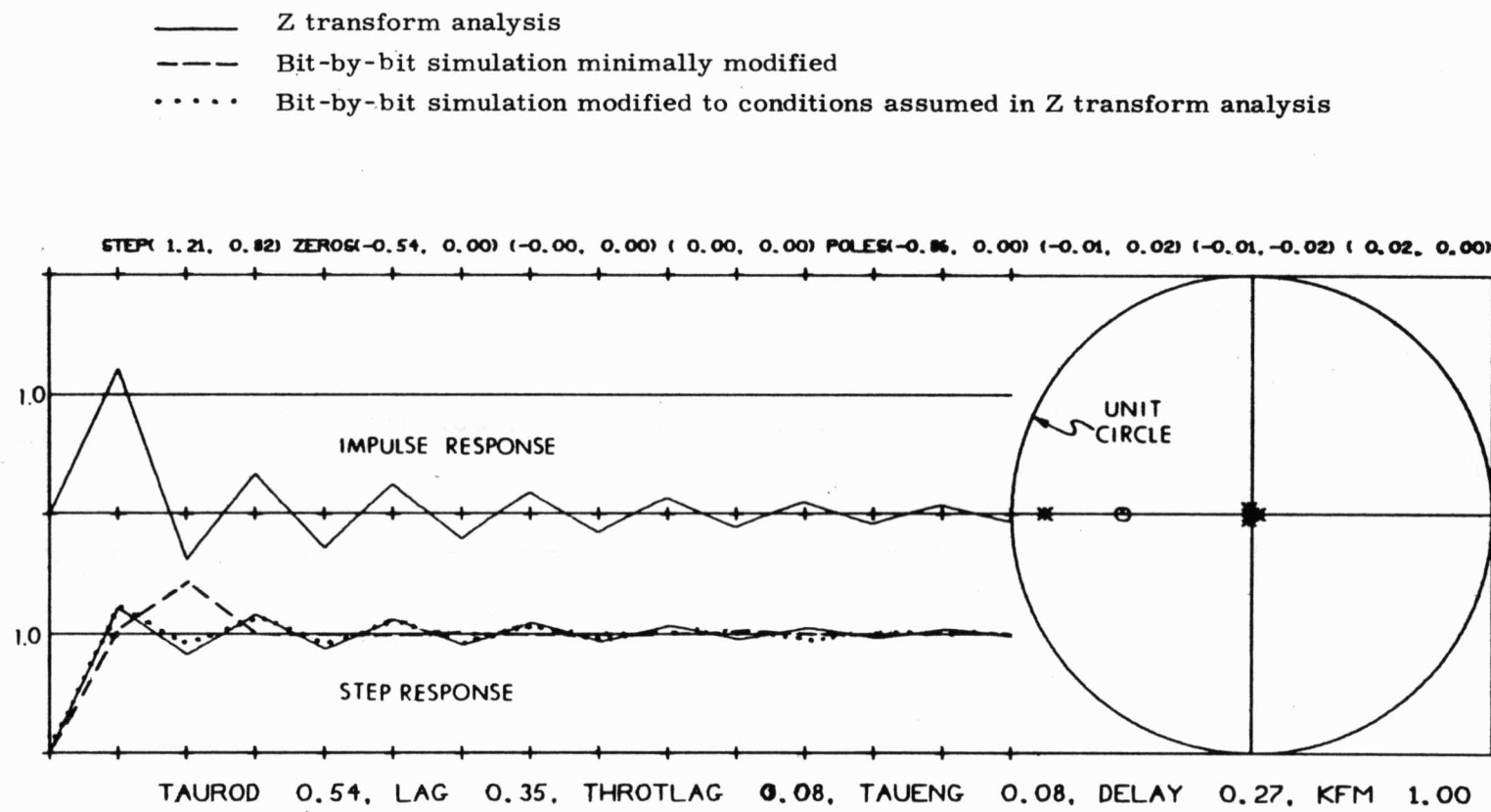


Fig. 15 Performance and roots at LO TAUROD.

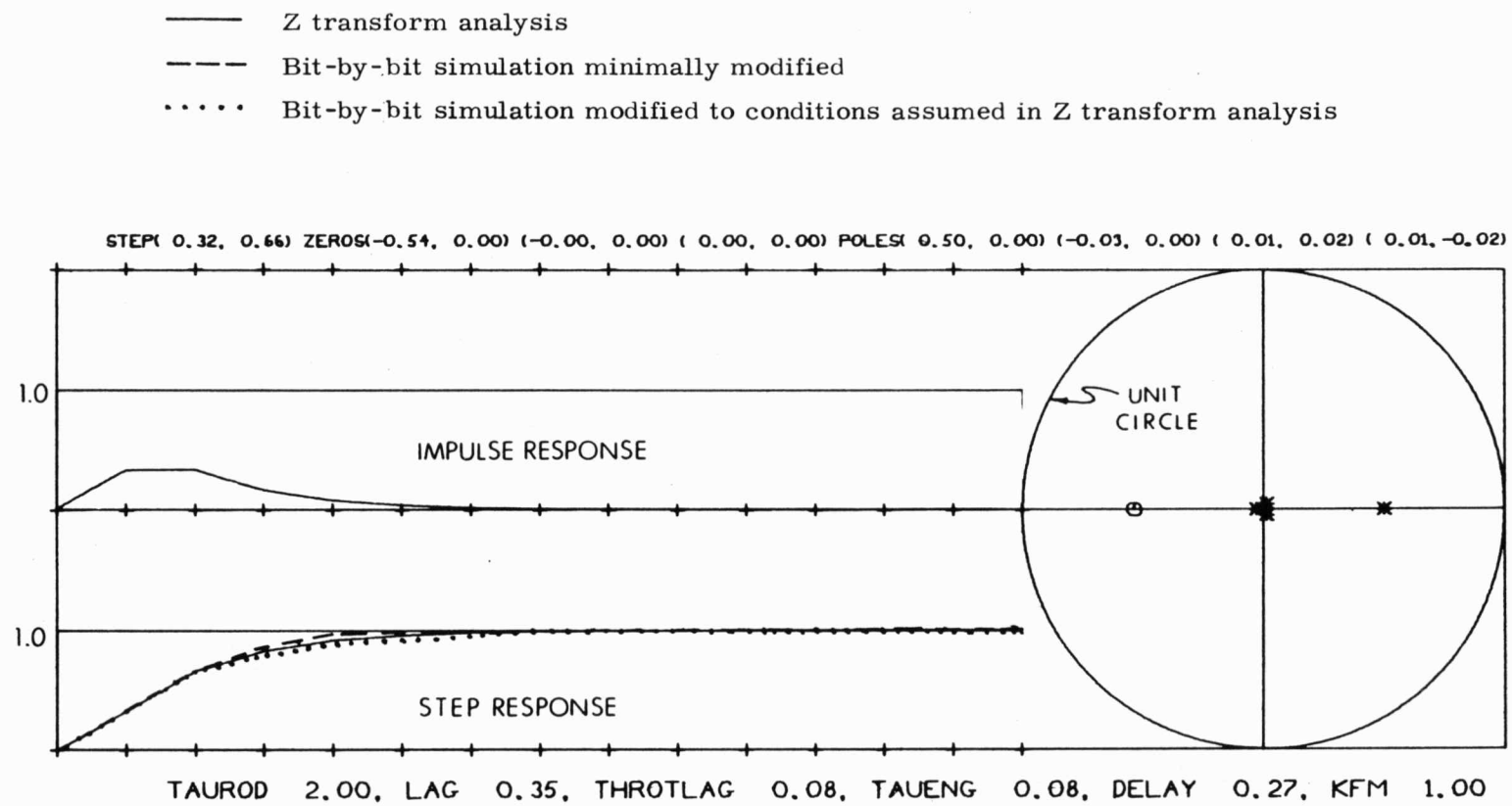


Fig. 16 Performance and roots at HI TAUROD.

- Z transform analysis
- - - Bit-by-bit simulation minimally modified
- · · · Bit-by-bit simulation modified to conditions assumed in Z transform analysis

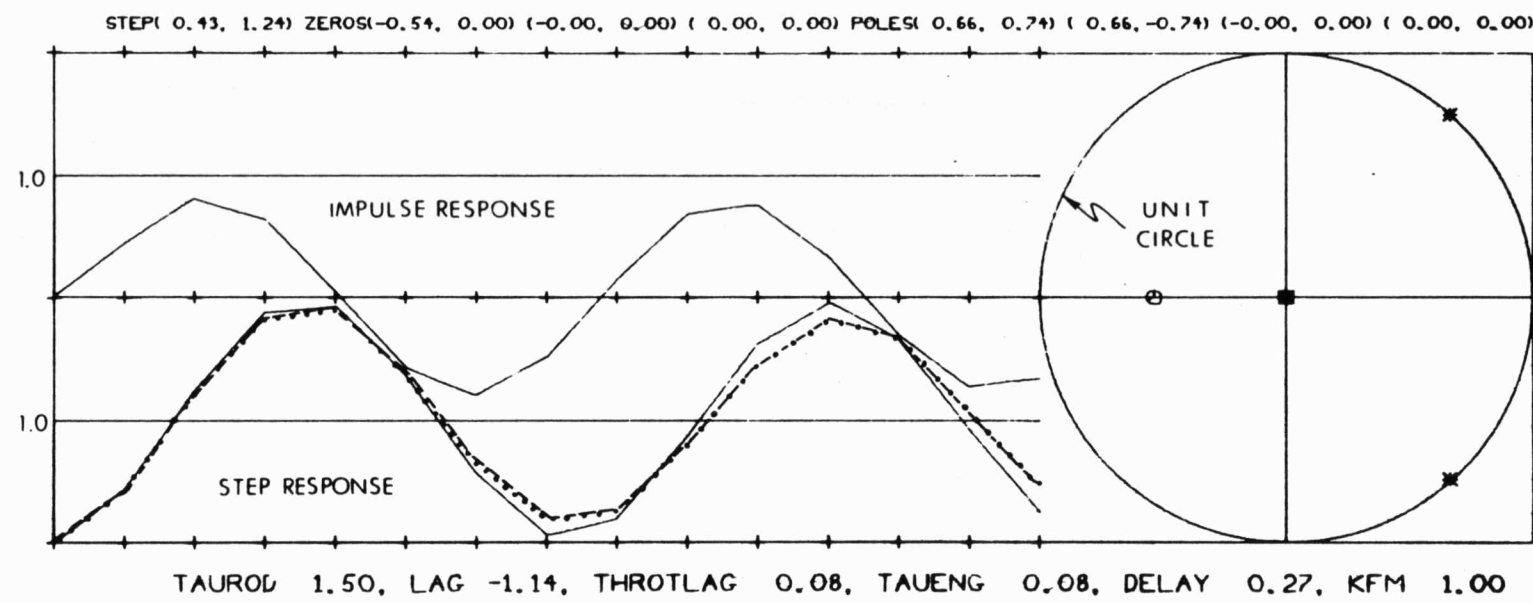


Fig. 17 Performance and roots at LO LAG.

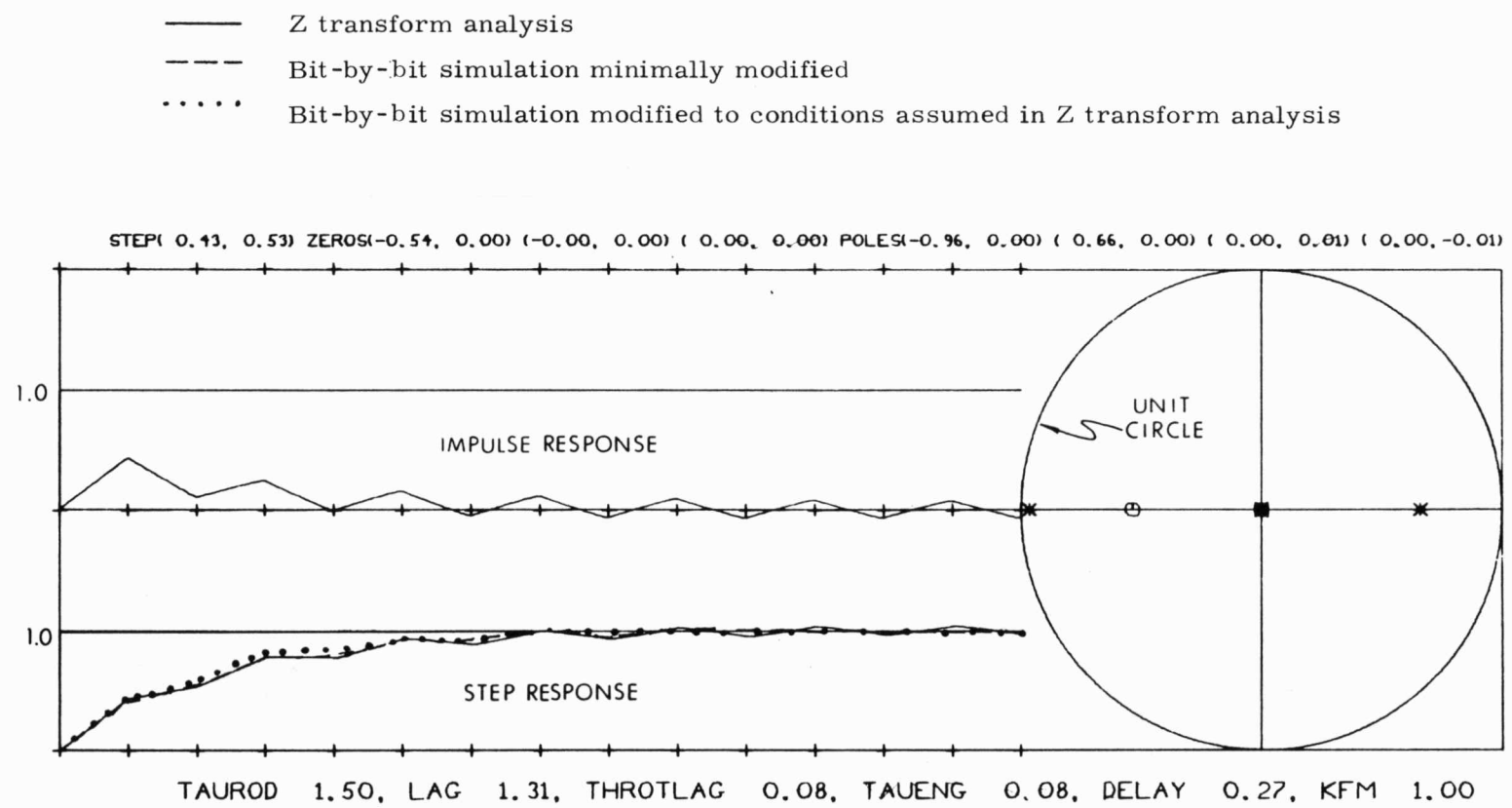


Fig. 18 Performance and roots at HI LAG.

- Z transform analysis
- - - Bit-by-bit simulation minimally modified
- · · Bit-by-bit simulation modified to conditions assumed in Z transform analysis

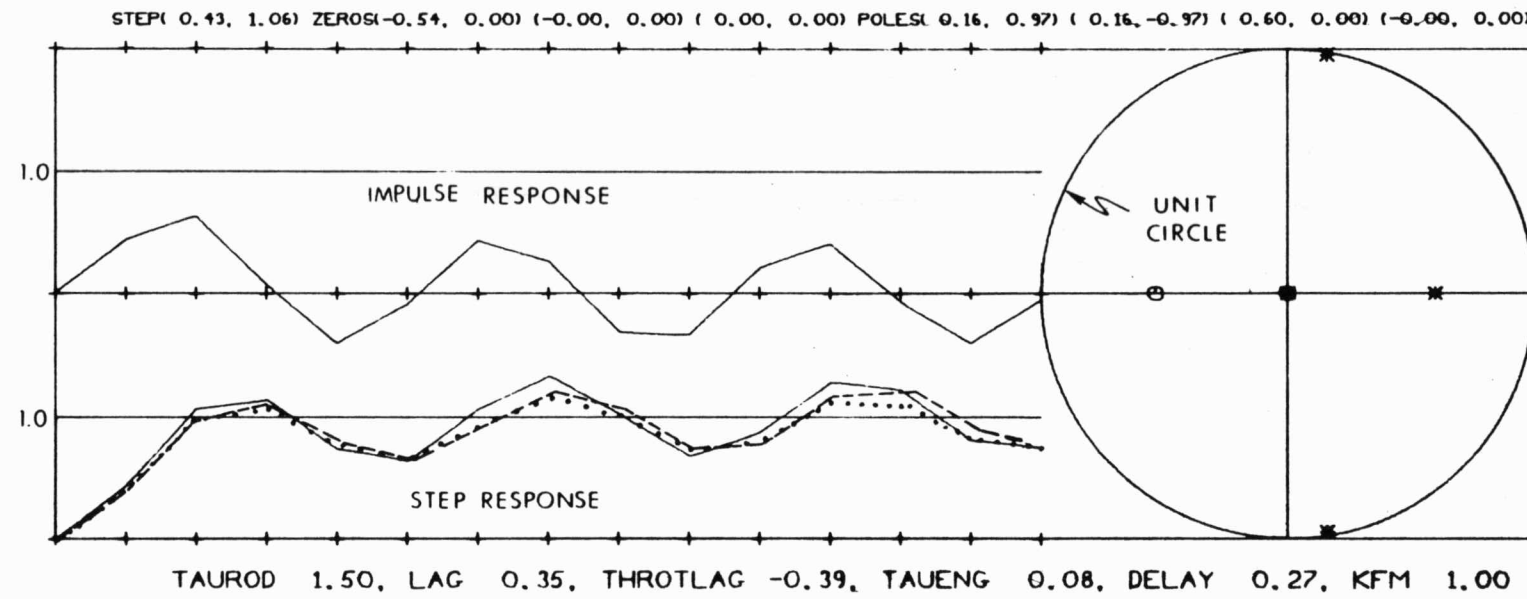


Fig. 19 Performance and roots at LO THROTLAG.

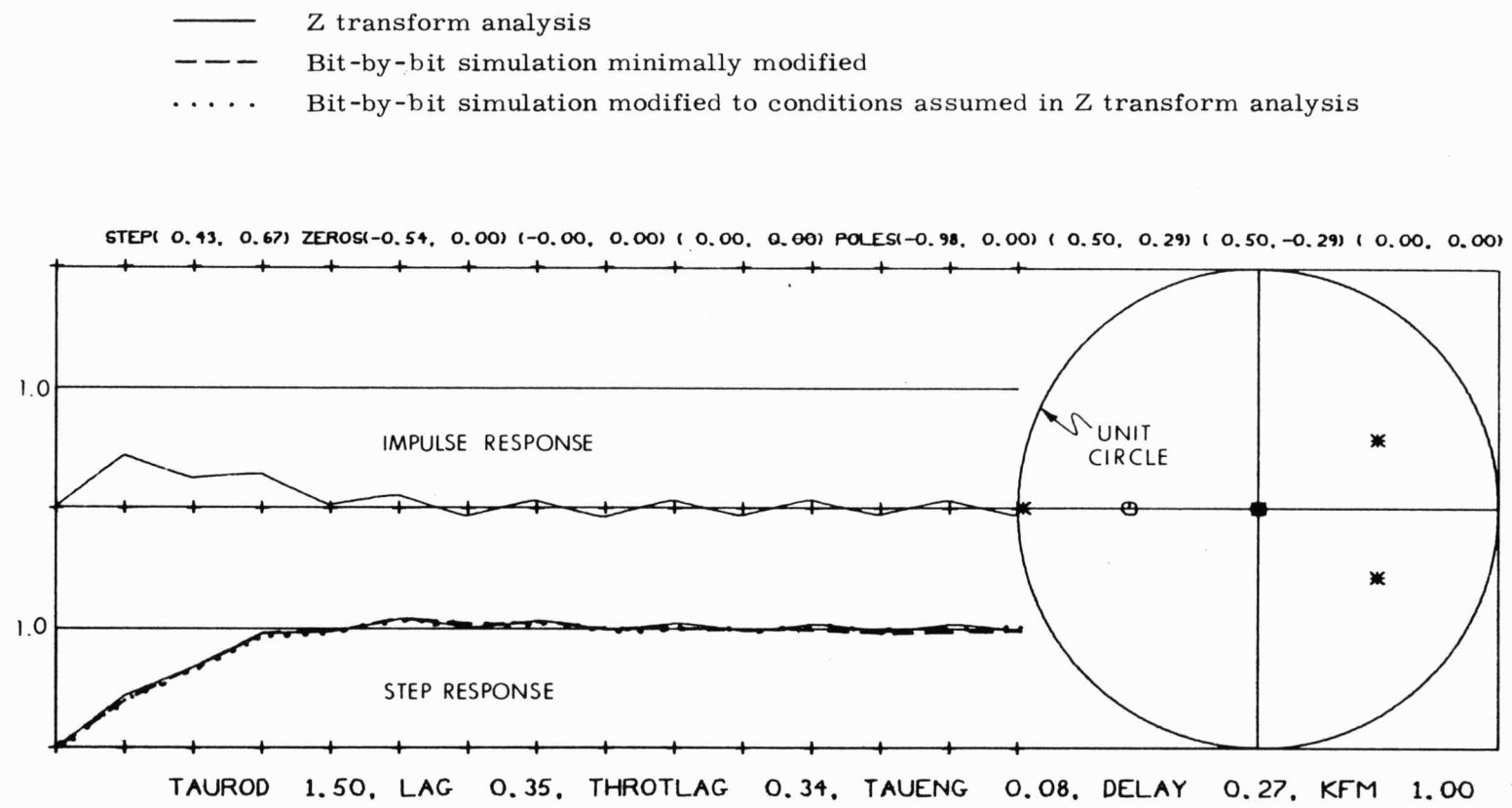


Fig. 20 Performance and roots at HI THROTLAG.

- Z transform analysis
- - - Bit-by-bit simulation minimally modified
- Bit-by-bit simulation modified to conditions assumed in Z transform analysis

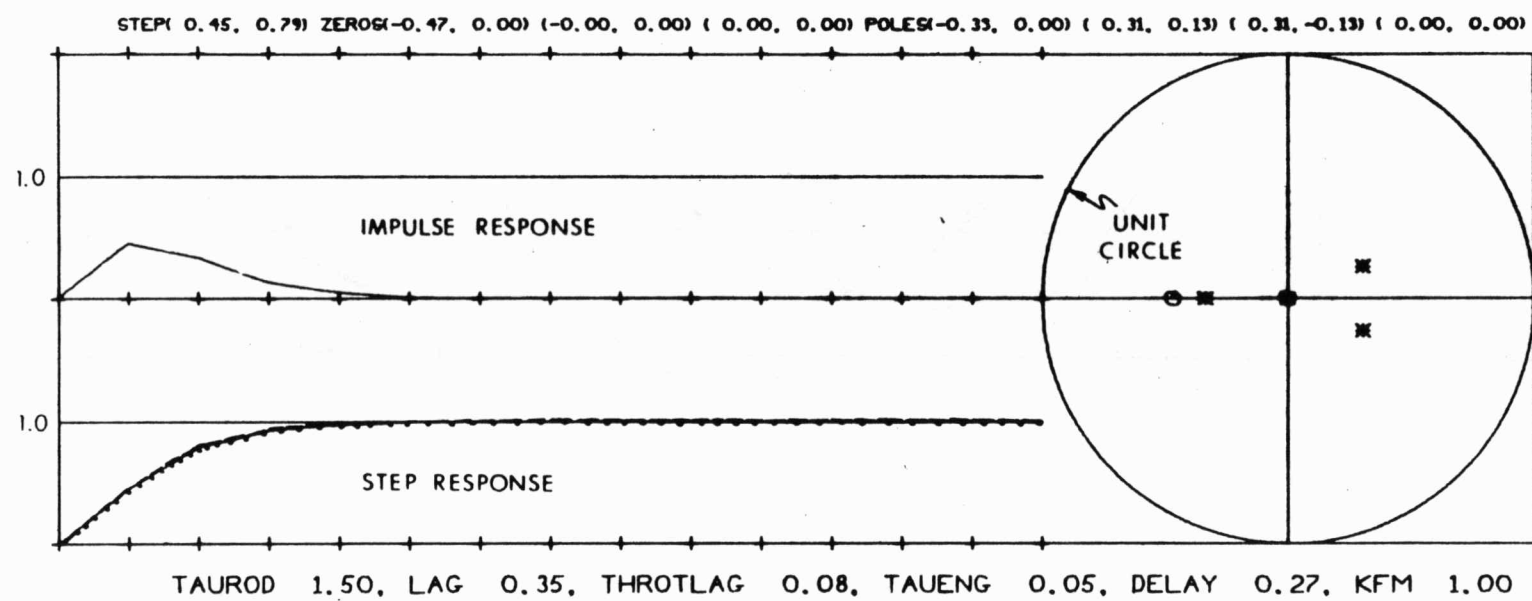


Fig. 21 Performance and roots at LO TAUENG.

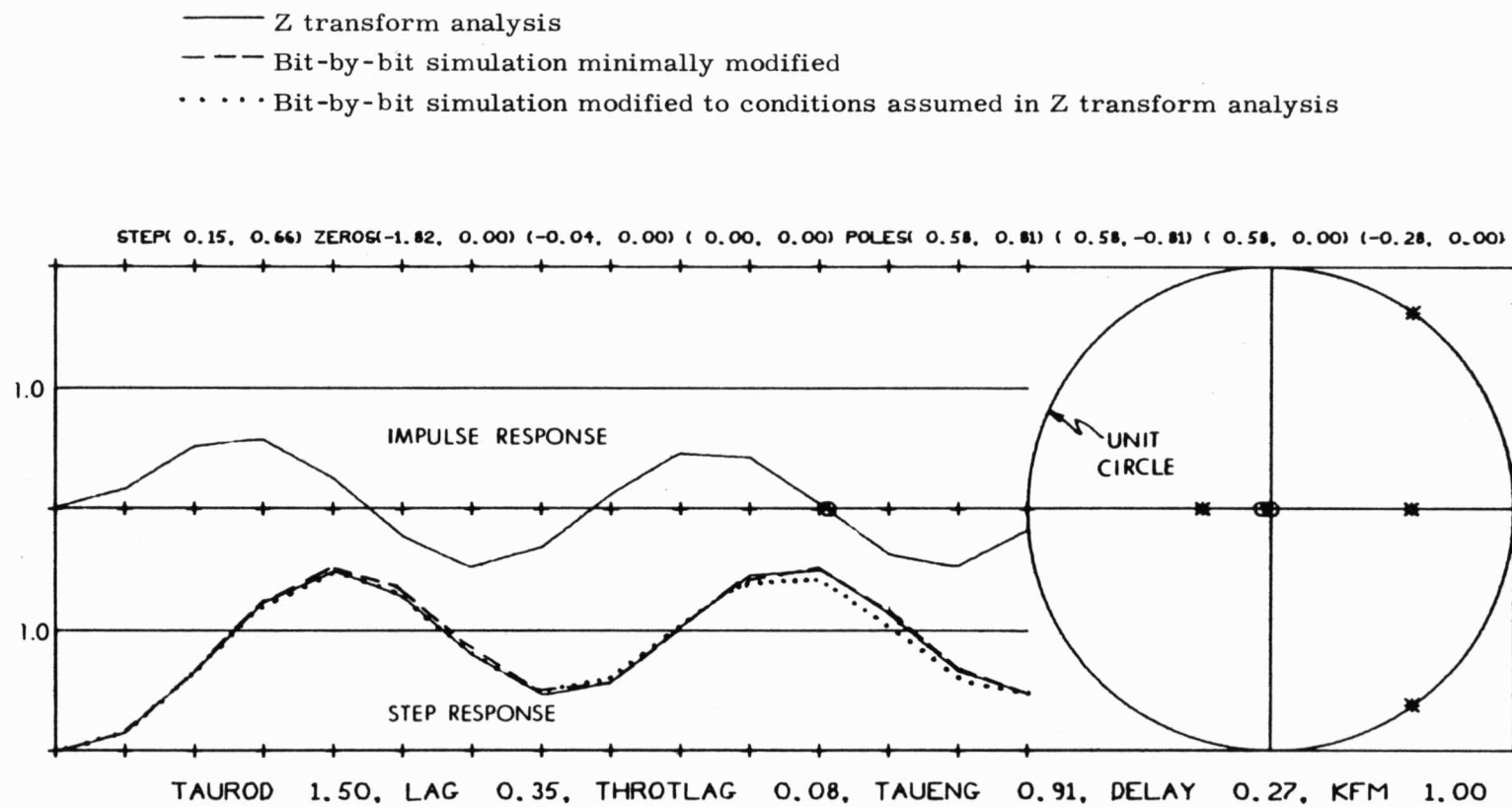


Fig. 22 Performance at HI TAUENG.

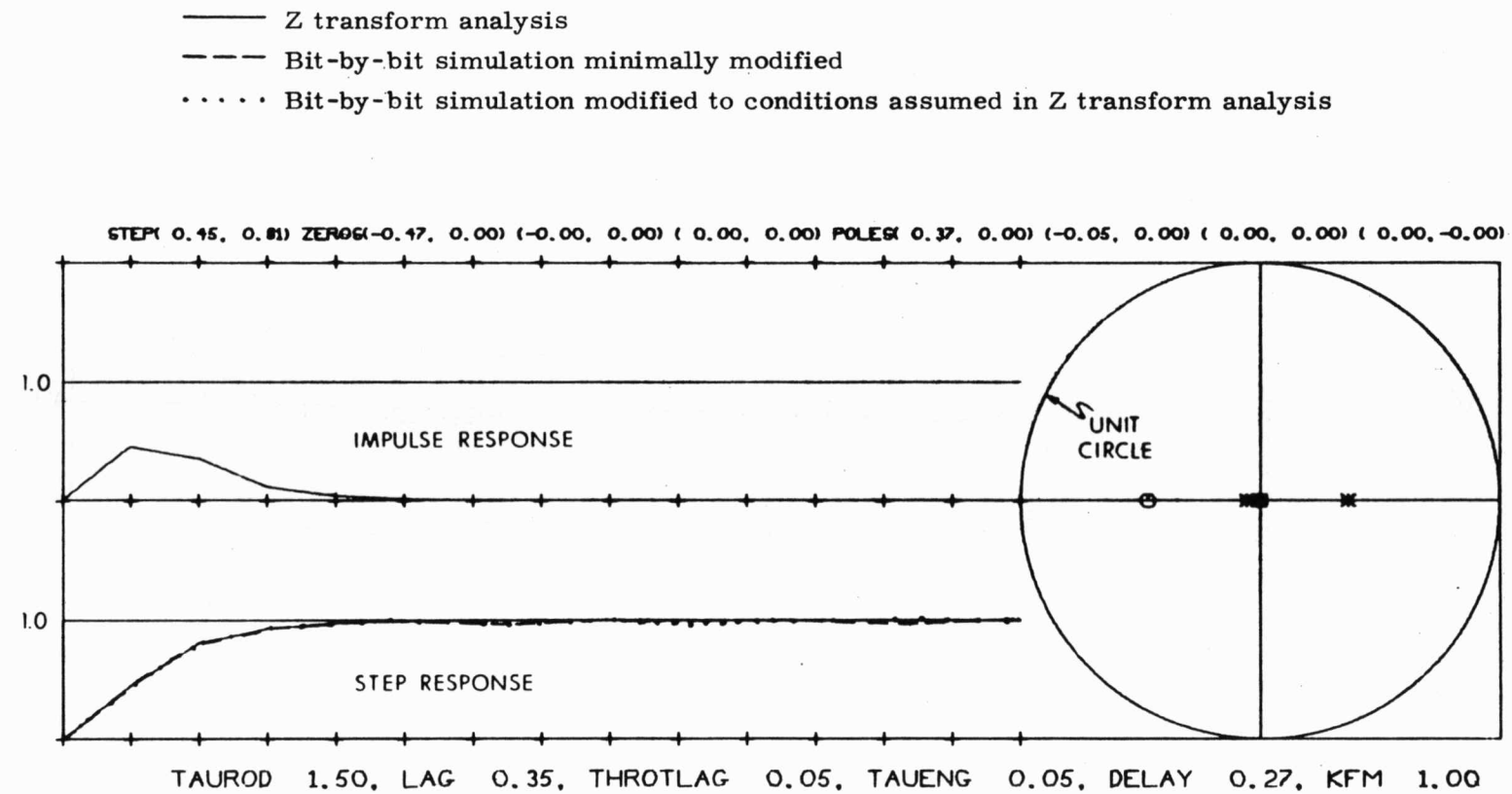


Fig. 23 Performance and roots at parameter settings equivalent to LO DELAY.

——— Z transform analysis
 - - - Bit-by-bit simulation minimally modified
 · · · Bit-by-bit simulation modified to conditions assumed in Z transform analysis

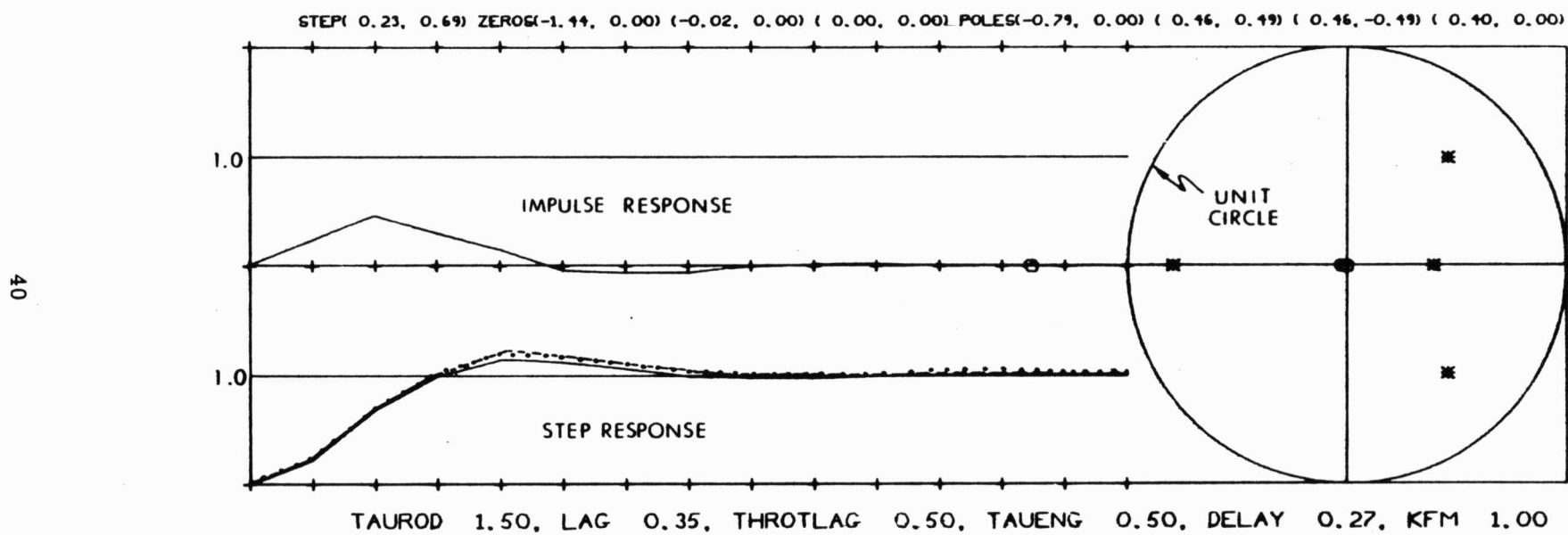


Fig. 24 Performance and roots at parameter settings equivalent to HI DELAY.

——— Z transform analysis
 - - - Bit-by-bit simulation minimally modified
 · · · Bit-by-bit simulation modified to conditions assumed in Z transform analysis

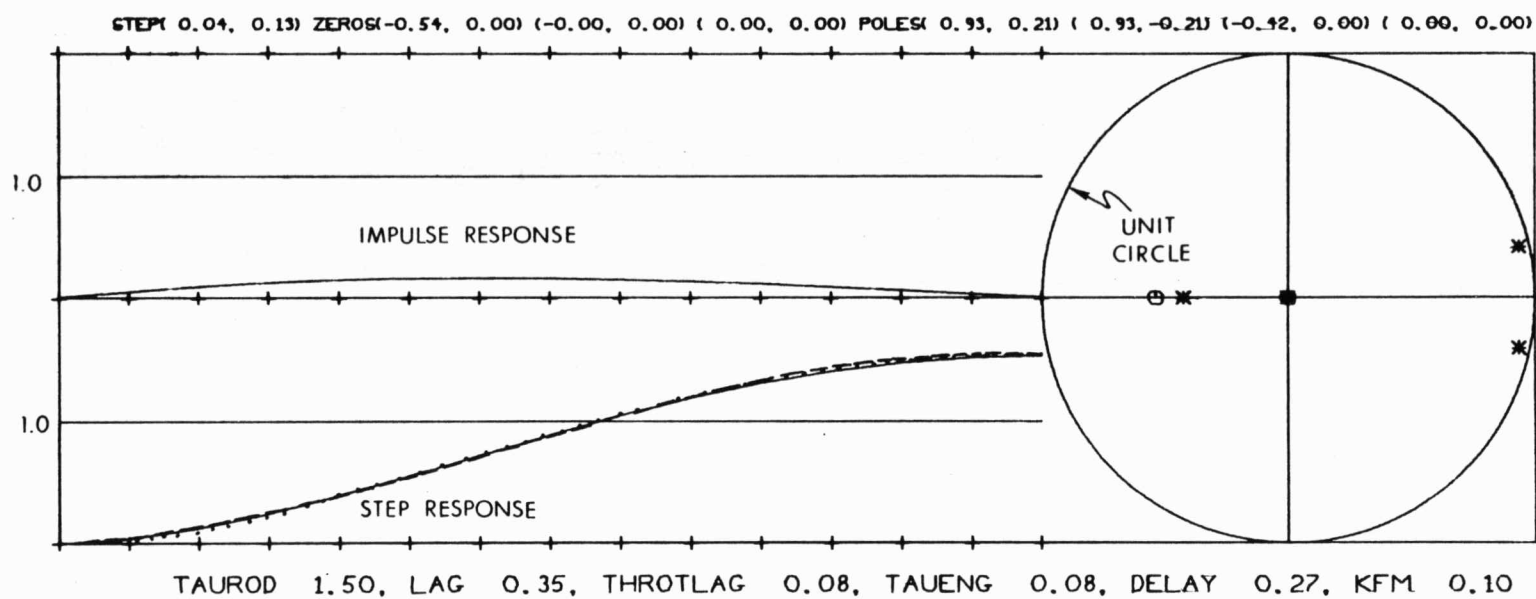


Fig. 25 Performance and roots at LO KFM.

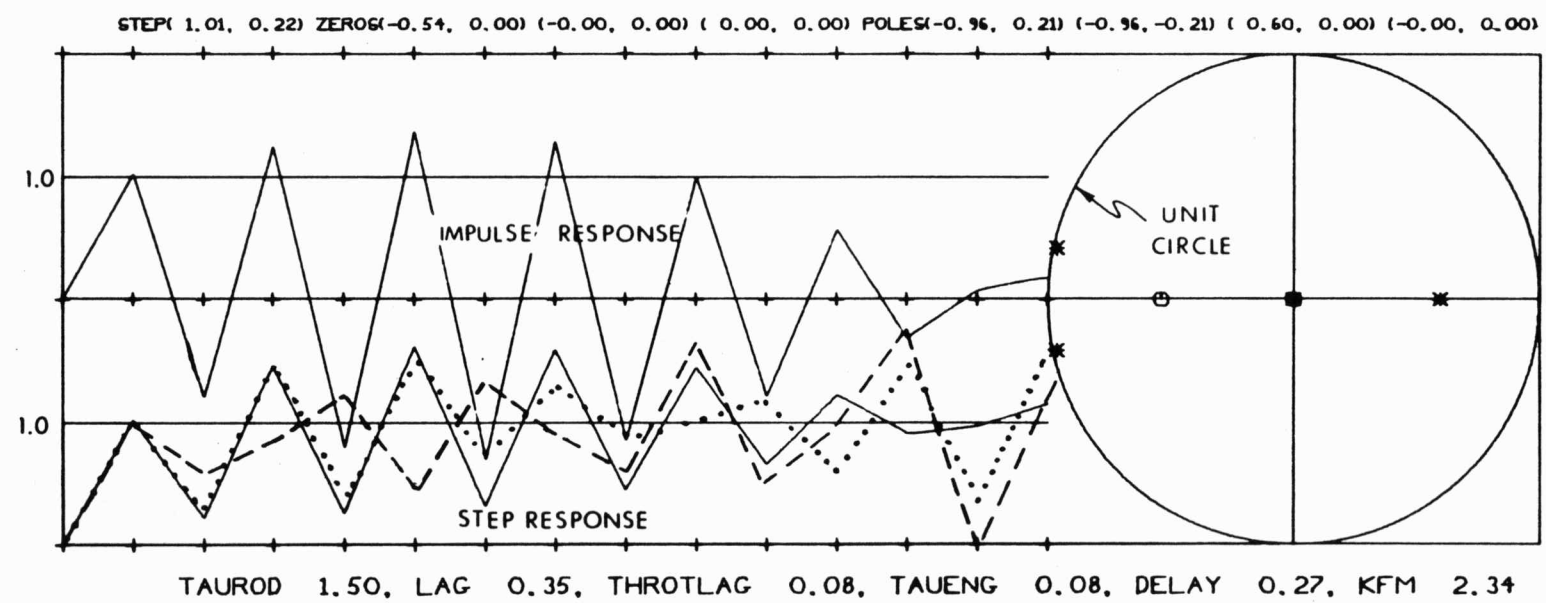


Fig. 26 Performance and roots at HI KFM.

REFERENCES

1. Schindwolf, R., "Rate of Descent (ROD) Mode Stability and Performance Analysis", Grumman Aerospace Corporation LM Memo, LM0-500-767, July 6, 1970.
2. Sorensen, J.A., "Linear Stability Analysis of LM Rate-of-Descent Guidance Equations Case 310", BELLCOMM, Inc., B70 06074, June 25, 1970.
3. Suddath, J., "P-66 Stability Analysis", National Aeronautics and Space Administration, Manned Spacecraft Center, EG2-70-100, July 1, 1970.
4. Guidance System Operations Plan for Manned LM Earth Orbital and Lunar Missions Using Program LUMINARY 1C (Rev. 130), R-567, Section 5, Guidance Equations (Rev. 7), Massachusetts Institute of Technology, Charles Stark Draper Laboratory, November 1969.
5. Baker, J., Crews, R., Marks, P., Tobey, R. and Victor, K., "PL/I FORMAC INTERPRETER USER'S REFERENCE MANUAL", IBM-Boston Programming Center, October 16, 1967.
6. Blair-Smith, Hugh, "AGC4 Memo #9 - Block II Instructions", MIT Instrumentation Laboratory, September 30, 1965, Revised June 1, 1967.

APPENDIX A

DERIVATION OF THE ACCELERATION CORRECTION INCREMENT

Figure A1 shows the model used to derive the acceleration correction increment. All time delays pertaining to the ROD guidance algorithm and to the throttle program are defined there. The DECA (Descent Engine Control Assembly) delay TD is the time required to issue the throttle command pulses at the rate of 3200 pulses per second. The engine response is assumed to be a pure delay of TT.

The object is to determine the acceleration correction increment δA_P which must be added to the average acceleration computed from the accelerometer readings \tilde{A} such as to yield actual acceleration at the current sample instant A_A . (This is the final acceleration of the preceding sample interval.) The average acceleration computed from the accelerometer readings during the sample interval T can be obtained by inspection of Fig. A1 as:

$$\tilde{A} = \frac{A_0(TC + TT) + A_A(T - TC - TT - TD) + (A_0 + A_A)TD/2}{T}.$$

The initial acceleration of the preceding sample interval is

$$A_0 = A_A - \delta A_C.$$

The acceleration correction increment is defined as

$$\delta A_P = A_A - \tilde{A}.$$

Substituting these last two expressions into the first yields

$$\delta A_P = \frac{A_A T - (A_A - \delta A_C)(TC + TT) - A_A(T - TC - TT - TD) - (2A_A - \delta A_C)TD/2}{T}.$$

This reduces immediately to

$$\delta A_P = \delta A_C \frac{TC + TT + TD/2}{T}.$$

$TC + TD/2$ is the computed delay D. Thus the acceleration correction increment is computed as

$$\delta A_P = \delta A_C \frac{D + TT}{T},$$

as shown in the block diagrams (Figs. 5 - 7).

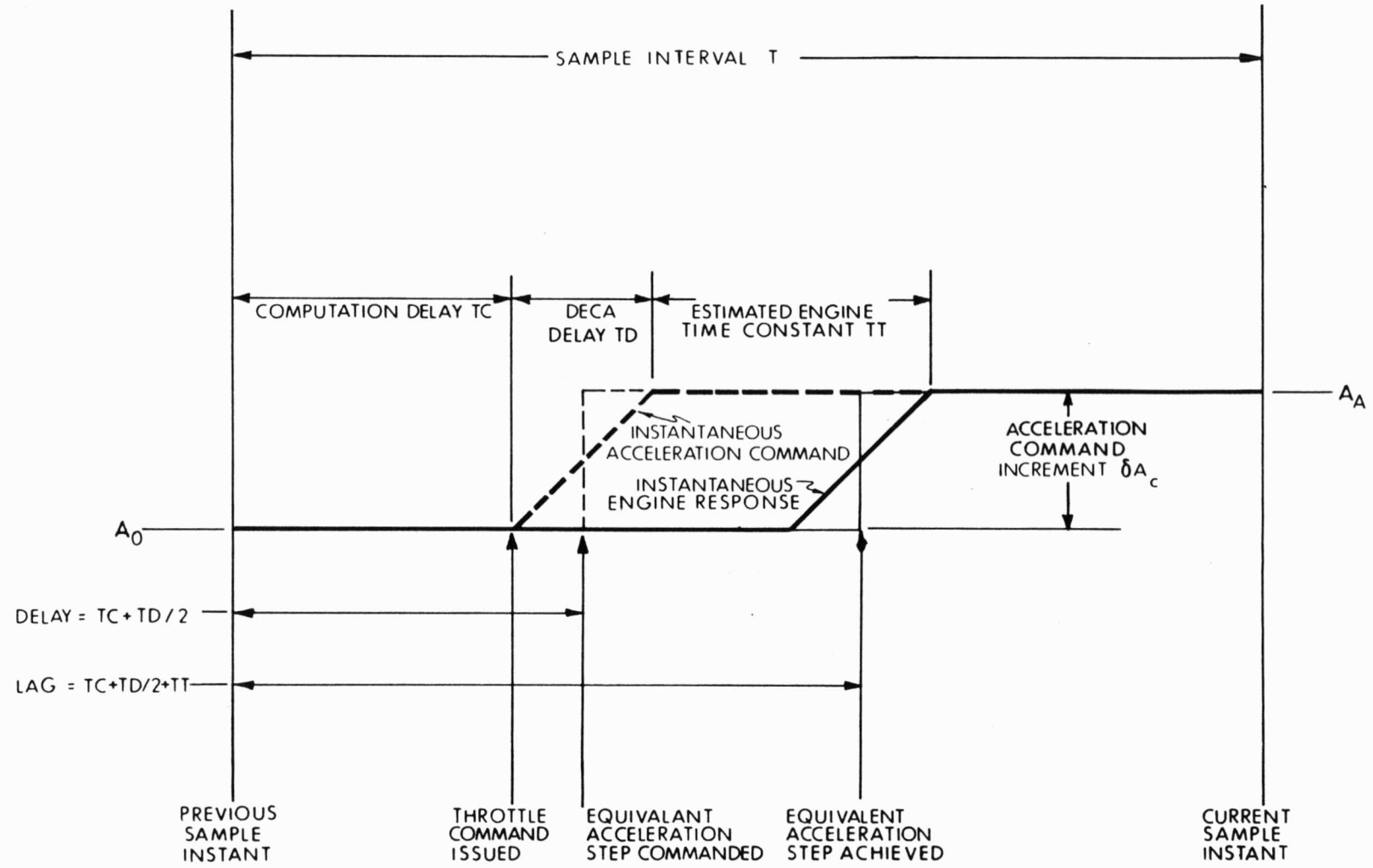


Fig. A1 Acceleration Response Model Used in Deriving the Acceleration Correction Increment δA_p

APPENDIX B

POLE-ZERO POLYNOMIAL COEFFICIENTS

Expressions for the coefficients of the pole and zero polynomials were derived using a FORMAC program (FORMAC is an IBM processor which symbolically manipulates algebraic equations. See Ref. 5). These expressions use the abbreviated nomenclature.

Table B1 lists the coefficients of the polynomial of the system zeros, CZ_3 thru CZ_0 and the polynomial of the system poles, CP_4 thru CP_0 , with the engine modeled as a first order lag. The coefficients of Table B1 are consistent with the block diagram of Fig. 7. The coefficients of the zero polynomial are defined, for example, as

$$CZ_3 Z^3 + CZ_2 Z^2 + CZ_1 Z + CZ_0 = 0.$$

Table B2 lists the coefficients of the polynomials with the engine modeled as a pure time delay. For this case the block diagram of Fig. 7 is modified by the substitution

$$G_3 = \frac{KFM \left[(D + TE) Z + (T - D - TE) Z^2 \right]}{(Z - 1)^2}.$$

It can be demonstrated that the coefficients of Table B2 are identical to those produced by Schindwolf (Ref. 1) when the appropriate correspondences are introduced. It is also easy to verify that exact compensation produces the simplified results reported by Schindwolf. If an equivalent system model is obtained by letting D' represent the computation delay plus half the DECA delay plus the engine delay so that

$$D' = D + TE = D + TT = LAG = .35 \text{ second},$$

and

$$TV = 1.5 \text{ second},$$

$$KFM = 1,$$

then in this special case the zero polynomial reduces to

$$(T - D') Z + D' = 0,$$

and the pole polynomial reduces to

$$TV Z^2 + (T - TV) Z = 0.$$

Thus there remains a zero on the negative real axis at $-D'/(T - D')$, a single pole at the origin, and a single pole on the positive real axis at $(TV - T)/TV$. For the parameters assumed the zero lies at $-.538$ and the pole is at $+1/3$.

The simplification immediately suggests choosing TV such as to cancel the non-zero zero with the non-zero pole. For cancellation we would have

$$(TV - T)/TV = -D'/(T - D')$$

which produces the obvious solution

$$TV = T - D'.$$

That is, if the descent engine responds as a pure delay, then the response of the total system is exactly equivalent to a pure delay D' . The time remaining in the sample interval to null the extrapolated velocity error is simply $T - D'$. With the inverse gain setting $TV = T - D'$ the error will be zero at all succeeding sample instants. Unfortunately, the error will not be zero between sample instants. Based on the first-order-lag engine model, Figure B1 shows that this value of TAURON produces overshoot between the sample instants while maintaining zero error at the sample instants.

CZ = -TE KFM+EA TE KFM+T KFM-D KFM
 3

CZ = TE KFM ET-T KFM ET+D KFM ET+TE KFM-2 EA TE KFM+D KFM
 2

CZ = -TE KFM ET-D KFM ET+EA TE KFM
 1

CZ = 0
 0

CP = TV
 4

CP = -2 TV-TE KFM K+EA TE KFM K+T KFM K-D KFM K+D K+TT K-TV ET
 3

-TE KFM+EA TE KFM+T KFM-D KFM

CP = TV+TE KFM ET K-T KFM ET K+D KFM ET K-D ET K-TT ET K
 2

-3 EA TE KFM K+2 TE KFM K-T KFM K+2 D KFM K
 -2 D K-2 TT K+TE KFM ET-T KFM ET+D KFM ET+2 TV ET
 +TE KFM-2 EA TE KFM+D KFM

CP = -2 TE KFM ET K+T KFM ET K-2 D KFM ET K+2 D ET K+2 TT ET K
 1

-TE KFM K+3 EA TE KFM K-D KFM K+D K
 +TT K-TE KFM ET-D KFM ET-TV ET+EA TE KFM

CP = TE KFM ET K+D KFM ET K-D ET K-TT ET K-EA TE KFM K
 0

Table B1 Coefficients of the Closed Loop System Poles and Zeros with the Engine Modeled as a First Order Lag

CZ₂ = -D KFM-TE KFM+T KFM
 CZ₁ = D KFM+TE KFM
 CZ₀ = 0
 CP₃ = TV
 CP₂ = -2 TV-D KFM-K D KFM-TE KFM-K TE KFM+T K KFM+T KFM+K D+K TT
 CP₁ = TV+D KFM+2 K D KFM+TE KFM+2 K TE KFM-T K KFM-2 K D-2 K TT
 CP₀ = -K D KFM-K TE KFM+K D+K TT

Table B2 Coefficients of the Closed Loop System Poles and Zeros with the Engine Modeled as a Pure Time Delay

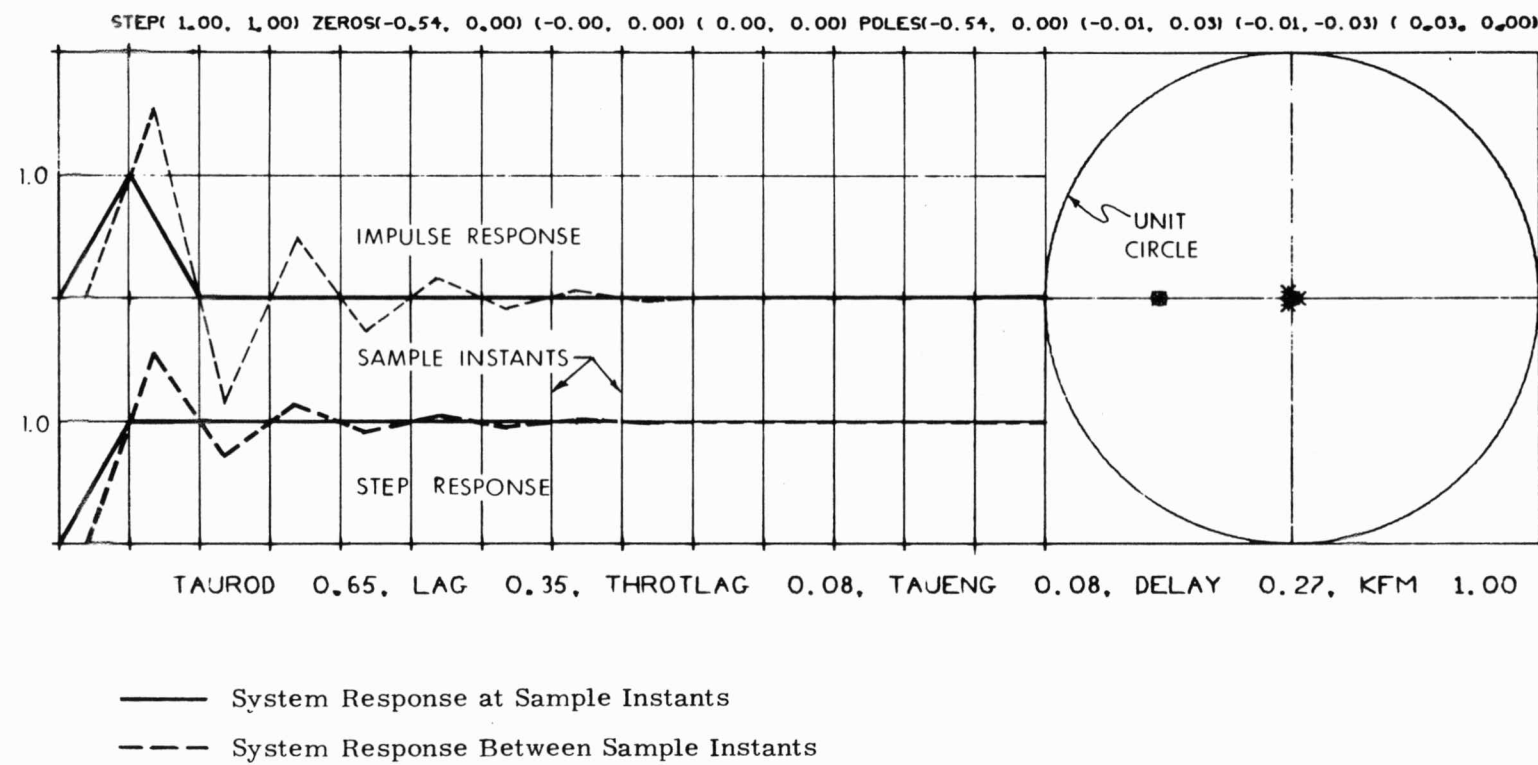


Fig. B1 Performance and roots for pole-zero cancellation.

APPENDIX C

CONDITIONS FOR BIT-BY-BIT SIMULATIONS

These notes are based on the routines of revision 167 of the LGC program LUMINARY. The LGC instructions are defined by Ref. 6.

Conditions for All Bit-By-Bit Simulation Step Responses

1. Radar noise was eliminated by altering the LGC SERVICER routine such that the state vector updated by the Average G equations was never replaced by the state vector further updated by the radar.
2. The step change in the altitude rate command is 2 fps.
3. In the two HI KFM cases fuel slosh was not simulated in order to avoid numerical problems in the slosh simulation. In all but the two HI KFM cases, fuel slosh was simulated.
4. At READACCS time(the time at which the accelerometers are read in the SERVICER routine) preceding the step input, the environment mass was 7851.863 KG.

Conditions for The Minimally Modified Bit-by-Bit Simulation Step Responses

1. At READACCS time preceding the step input the LGC mass was 7781.095 KG, 0.9% lower than the environment mass.
2. The inverse sensitivity of the engine was .079796 bits per newton (GSOP value Ref. 4) in the environment and in the LGC, except in the LO KFM cases where the environment inverse sensitivity was divided by the indicated KFM.
3. With the above parameters, the time required to output the throttle bits was sufficient to cause the bit-by-bit results to differ considerably from the Z transform results in several cases. This is especially noticeable in the LO TAUROD case Fig. 15 and in the HI KFM case Fig. 26. The following table illustrates the equivalent system time delay due to outputting throttle bits on the first

and second passes for some typical cases. The equivalent system delay is half the time required to output the throttle bits at 3200 bits/second.

CASE	PASS	BITS	Equivalent System Delay (ms)
NOMINAL	First	243	38
	Second	-153	24
LO TAURD	First	685	107
	Second	-1157	181
HI KFM	First	243	38
	Second	-551	86

4. In the LO (negative) THROTLAG case, it was necessary to modify the LGC throttle routine's calculation of FWEIGHT. The LGC program subtracts the time of the P66 accelerometer reading from the current clock reading, adds THROTLAG, and then takes the absolute value. (Taking the absolute value corrects for a change in the high order clock word, only the low order clock readings are used.) This order of computations produces a positive result even when THROTLAG is sufficiently negative so that the result should be negative. To produce the correct result, the order of LGC computations was interchanged by taking the absolute value of the clock difference first and then adding THROTLAG.

Conditions for the Bit-by-Bit Simulations Modified to Adherer to the Conditions of the Z Transform Analysis

1. At READACCS time preceding the step input the LGC mass was set identical to the environment mass.
2. The inverse sensitivity of the engine was .0079796 bits per newton (1/10 of GSOP value) in the environment and in the LGC, except in the LO KFM and HI KFM cases where the environment sensitivity was divided by the indicated KFM.

3. With the above parameters, the time required to output the throttle bits was considerably reduced compared to the minimally modified runs so that the bit-by-bit simulation results adhere much more closely to the Z transform analysis results. The following table illustrates the equivalent system time delay due to outputting throttle bits on the first and second passes for typical cases.

CASE	PASS	BITS	Equivalent System Delay
NOMINAL	First	24	3.750
	Second	-15	2.344
LO TAUROD	First	69	10.781
	Second	-130	20.312
HI KFM	First	24	3.750
	Second	-57	8.906

4. Several corrections to the computation of FWEIGHT in the throttle program were made in all cases in this group. These corrections were:
- A. As in item 4 of the previous group of cases, we interchanged the order of taking the absolute value of the clock difference and adding THROTLAG.
 - B. In the computation of the first two terms of FWEIGHT, the single precision DOUBLE was changed to the double precision DDOUBL to correct a mistake in the LGC coding which produces a significant error only in these cases of unrealistically high engine sensitivity. The maximum error is 294 newtons in the HI KFM case, 12.5 newtons in the LO KFM case, and 125 newtons in the other cases of this group.
 - C. In the computation of the final term of FWEIGHT, the order of multiply and divide was reversed to preserve significance in the results. With these corrections, the FWEIGHT computation (in the language defined by Ref. 6) reads:

```

CAF      2SECS
TS       Q
EXTEND
MP      BIT6

```

LXCH BUF +1
CS BUF
AD TIME1
MASK LOW8
AD THROTLAG
ZL
EXTEND
DV Q
EXTEND
MP PIF
DDOUBL
DXCH FWEIGHT
CCS PIF
AD ONE
TCF +2
AD ONE
ZL
EXTEND
DV BUF +1
EXTEND
MP PIF
DAS FWEIGHT

APPENDIX D

ANALYSIS OF FASTER SYSTEMS

There have been suggestions to increase the speed of the ROD guidance channel. However, studies for TAUROD = 1.2 and 1.0 indicate that such schemes are not desirable since improvements in response time cause a reduction in stability margins. The results of these studies are presented in tables D1 and D2 and in Figs. D1 - D20 in the same formats as those used in Table 1 and Figs. 9 - 14.

	INITIAL VALUE	LAST UNSTABLE VALUE	FIRST STABLE VALUE	LAST STABLE VALUE	FIRST UNSTABLE VALUE	FINAL VALUE
TAUROD	1.2	X	X	X	X	1.2
LAG	-1.2	- .879	- .814	1.05	1.11	1.37
THROTLAG	- .41	- .352	- .333	.302	.322	.36
TAUENG	0	X	X	.721	.744	.93
DELAY	0	X	X	X	X	.92
KFM	.1	X	X	2.11	2.17	2.4

Table D1 STABILITY REGIONS OF EACH PARAMETER FOR TAUROD=1.2

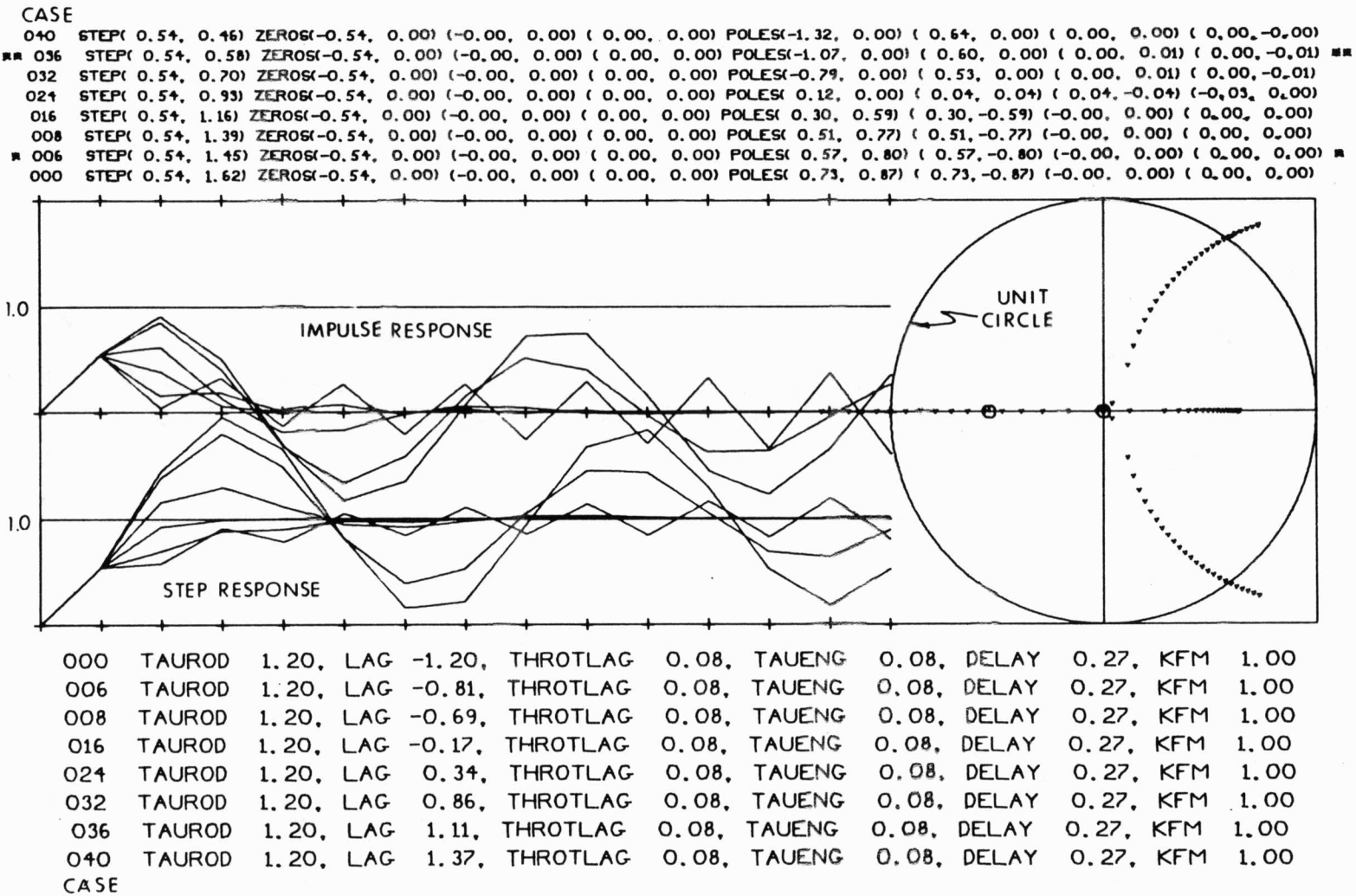
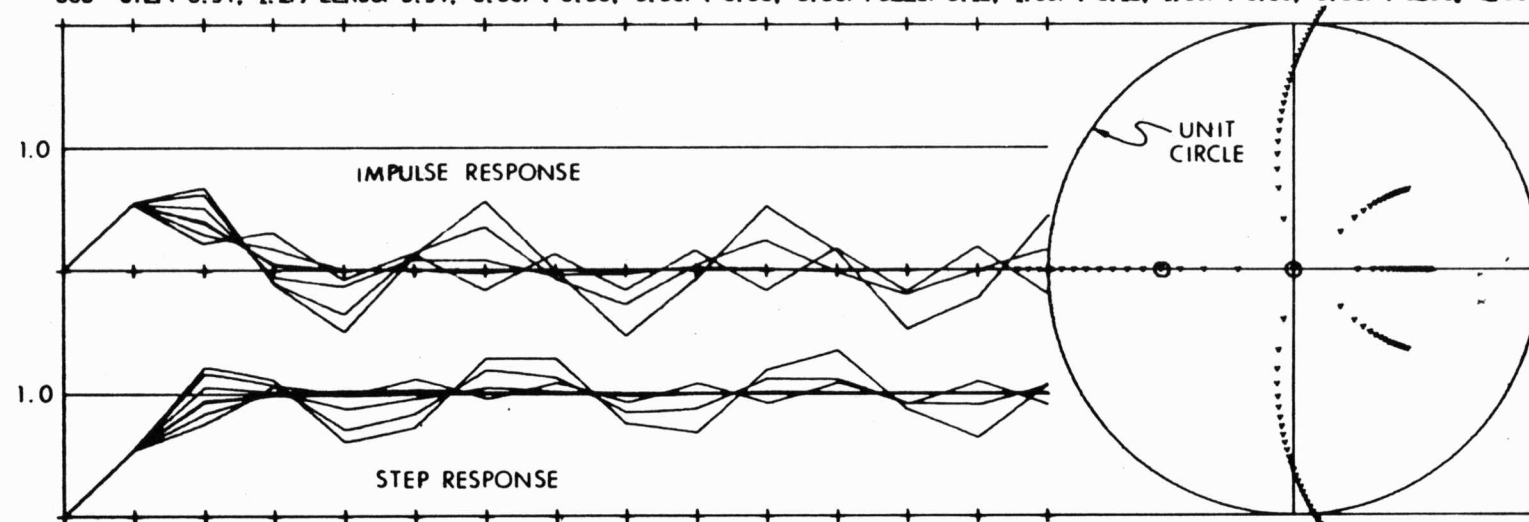


Fig. D1 Performance and roots vs LAG for TAUROD = 1.2.

CASE
 040 STEP(0.54, 0.73) ZEROS(-0.54, 0.00) (-0.00, 0.00) (0.00, 0.00) POLES(-1.12, 0.00) (0.46, 0.33) (0.46,-0.33) (0.00, 0.00)
 038 STEP(0.54, 0.75) ZEROS(-0.54, 0.00) (-0.00, 0.00) (0.00, 0.00) POLES(-1.04, 0.00) (0.45, 0.32) (0.45,-0.32) (0.00, 0.00)
 032 STEP(0.54, 0.84) ZEROS(-0.54, 0.00) (-0.00, 0.00) (0.00, 0.00) POLES(-0.74, 0.00) (0.37, 0.29) (0.37,-0.29) (0.00, 0.00)
 025 STEP(0.54, 0.93) ZEROS(-0.54, 0.00) (-0.00, 0.00) (0.00, 0.00) POLES(0.26, 0.00) (-0.04, 0.20) (-0.04,-0.20) (-0.00, 0.00)
 024 STEP(0.54, 0.94) ZEROS(-0.54, 0.00) (-0.00, 0.00) (0.00, 0.00) POLES(-0.06, 0.33) (-0.06,-0.33) (0.32, 0.00) (-0.00, 0.00)
 016 STEP(0.54, 1.05) ZEROS(-0.54, 0.00) (-0.00, 0.00) (0.00, 0.00) POLES(-0.03, 0.71) (-0.03,-0.71) (0.47, 0.00) (-0.00, 0.00)
 008 STEP(0.54, 1.16) ZEROS(-0.54, 0.00) (-0.00, 0.00) (0.00, 0.00) POLES(0.04, 0.91) (0.04,-0.91) (0.52, 0.00) (-0.00, 0.00)
 004 STEP(0.54, 1.21) ZEROS(-0.54, 0.00) (-0.00, 0.00) (0.00, 0.00) POLES(0.08, 0.99) (0.08,-0.99) (0.54, 0.00) (-0.00, 0.00)
 000 STEP(0.54, 1.27) ZEROS(-0.54, 0.00) (-0.00, 0.00) (0.00, 0.00) POLES(0.12, 1.06) (0.12,-1.06) (0.56, 0.00) (-0.00, 0.00)



000	TAUROD	1.20,	LAG	0.35,	THROTLAG	-0.41,	TAUENG	0.08,	DELAY	0.27,	KFM	1.00
004	TAUROD	1.20,	LAG	0.35,	THROTLAG	-0.33,	TAUENG	0.08,	DELAY	0.27,	KFM	1.00
008	TAUROD	1.20,	LAG	0.35,	THROTLAG	-0.26,	TAUENG	0.08,	DELAY	0.27,	KFM	1.00
016	TAUROD	1.20,	LAG	0.35,	THROTLAG	-0.10,	TAUENG	0.08,	DELAY	0.27,	KFM	1.00
024	TAUROD	1.20,	LAG	0.35,	THROTLAG	0.05,	TAUENG	0.08,	DELAY	0.27,	KFM	1.00
025	TAUROD	1.20,	LAG	0.35,	THROTLAG	0.07,	TAUENG	0.08,	DELAY	0.27,	KFM	1.00
032	TAUROD	1.20,	LAG	0.35,	THROTLAG	0.21,	TAUENG	0.08,	DELAY	0.27,	KFM	1.00
038	TAUROD	1.20,	LAG	0.35,	THROTLAG	0.32,	TAUENG	0.08,	DELAY	0.27,	KFM	1.00
040	TAUROD	1.20,	LAG	0.35,	THROTLAG	0.36,	TAUENG	0.08,	DELAY	0.27,	KFM	1.00

CASE

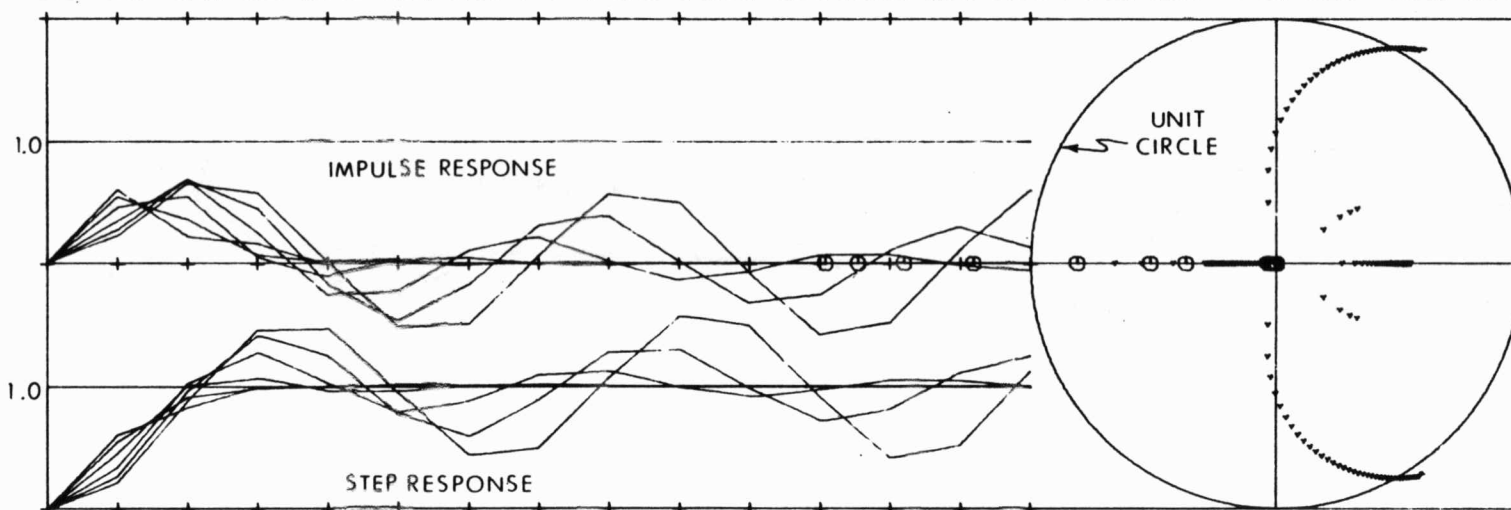
Fig. D2 Performance and roots vs THROTLAG for TAUROD = 1.2.

CASE

```

040 STEP( 0.19, 0.80) ZEROS(-1.84, 0.00) (-0.04, 0.00) ( 0.00, 0.00) POLES( 0.58, 0.87) ( 0.58,-0.87) ( 0.54, 0.00) (-0.29, 0.00)
■■ 032 STEP( 0.22, 0.88) ZEROS(-1.70, 0.00) (-0.03, 0.00) ( 0.00, 0.00) POLES( 0.49, 0.88) ( 0.49,-0.88) ( 0.52, 0.00) (-0.26, 0.00) ■■
024 STEP( 0.27, 0.96) ZEROS(-1.52, 0.00) (-0.03, 0.00) ( 0.00, 0.00) POLES( 0.37, 0.86) ( 0.37,-0.86) ( 0.50, 0.00) (-0.21, 0.00)
016 STEP( 0.34, 1.02) ZEROS(-1.23, 0.00) (-0.02, 0.00) ( 0.00, 0.00) POLES( 0.21, 0.80) ( 0.21,-0.80) ( 0.46, 0.00) (-0.13, 0.00)
008 STEP( 0.46, 1.01) ZEROS(-0.81, 0.00) (-0.00, 0.00) ( 0.00, 0.00) POLES( 0.02, 0.59) ( 0.02,-0.59) ( 0.39, 0.00) (-0.03, 0.00)
003 STEP( 0.55, 0.91) ZEROS(-0.51, 0.00) (-0.00, 0.00) ( 0.00, 0.00) POLES(-0.24, 0.00) ( 0.19, 0.14) ( 0.19,-0.14) ( 0.00, 0.00)
000 STEP( 0.61, 0.83) ZEROS(-0.37, 0.00) ( 0.00, 0.00) ( 0.00, 0.00) POLES(-0.66, 0.00) ( 0.33, 0.22) ( 0.33,-0.22) ( 0.00, 0.00)

```



```

000 TAUROD 1.20, LAG 0.35, THROTLAG 0.08, TAUENG 0.00, DELAY 0.27, KFM 1.00
003 TAUROD 1.20, LAG 0.35, THROTLAG 0.08, TAUENG 0.07, DELAY 0.27, KFM 1.00
008 TAUROD 1.20, LAG 0.35, THROTLAG 0.08, TAUENG 0.19, DELAY 0.27, KFM 1.00
016 TAUROD 1.20, LAG 0.35, THROTLAG 0.08, TAUENG 0.37, DELAY 0.27, KFM 1.00
024 TAUROD 1.20, LAG 0.35, THROTLAG 0.08, TAUENG 0.56, DELAY 0.27, KFM 1.00
032 TAUROD 1.20, LAG 0.35, THROTLAG 0.08, TAUENG 0.74, DELAY 0.27, KFM 1.00
040 TAUROD 1.20, LAG 0.35, THROTLAG 0.08, TAUENG 0.93, DELAY 0.27, KFM 1.00
CASE

```

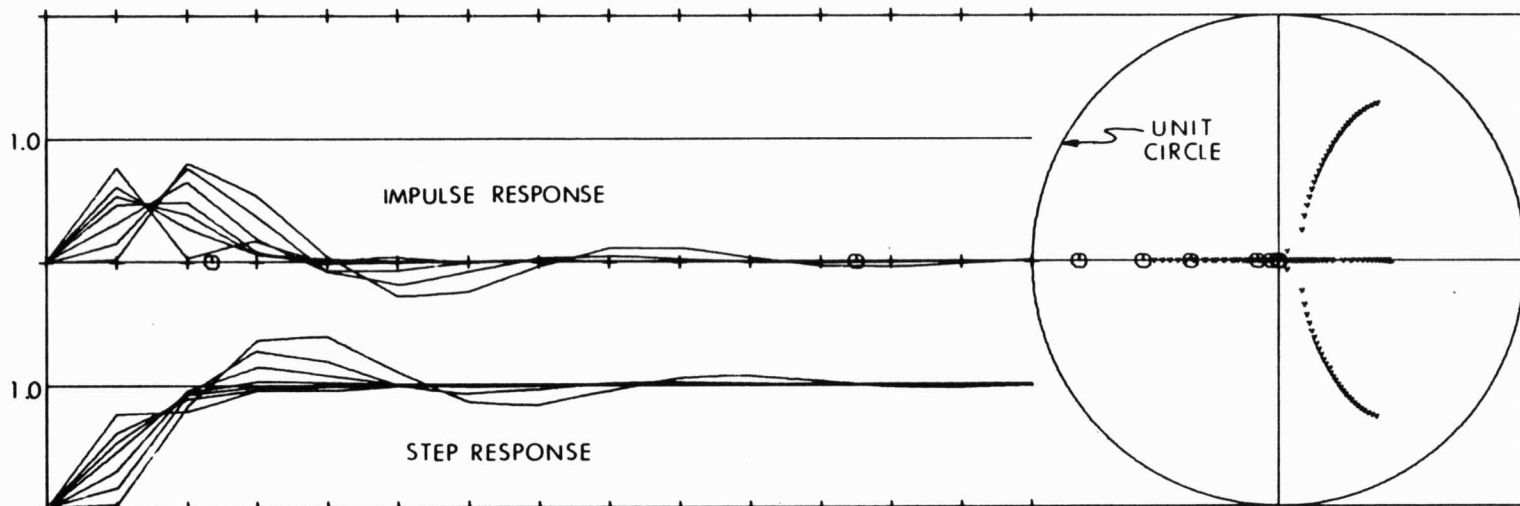
Fig. D3 Performance and roots vs TAUENG for TAUROD = 1.2.

CASE

```

040 STEP( 0.02, 0.82) ZEROS(81.11, 0.00) (-0.03, 0.00) ( 0.00, 0.00) POLES( 0.40, 0.64) ( 0.40,-0.64) (-0.35, 0.00) ( 0.19, 0.00)
032 STEP( 0.16, 0.92) ZEROS(-4.33, 0.00) (-0.00, 0.00) ( 0.00, 0.00) POLES( 0.28, 0.56) ( 0.28,-0.56) (-0.11, 0.00) ( 0.09, 0.00)
024 STEP( 0.31, 0.96) ZEROS(-1.71, 0.00) (-0.00, 0.00) ( 0.00, 0.00) POLES( 0.20, 0.14) ( 0.20,-0.14) (-0.04, 0.00) ( 0.04, 0.00)
016 STEP( 0.16, 0.95) ZEROS(-0.81, 0.00) (-0.00, 0.00) ( 0.00, 0.00) POLES( 0.12, 0.26) ( 0.12,-0.26) (-0.02, 0.00) ( 0.02, 0.00)
012 STEP( 0.54, 0.93) ZEROS(-0.55, 0.00) (-0.00, 0.00) ( 0.00, 0.00) POLES( 0.14, 0.00) ( 0.03, 0.04) ( 0.03,-0.04) (-0.03, 0.00)
008 STEP( 0.61, 0.89) ZEROS(-0.36, 0.00) (-0.00, 0.00) ( 0.00, 0.00) POLES( 0.32, 0.00) (-0.22, 0.00) ( 0.00, 0.01) ( 0.00,-0.01)
000 STEP( 0.77, 0.79) ZEROS(-0.09, 0.00) ( 0.00, 0.00) ( 0.00, 0.00) POLES(-0.50, 0.00) ( 0.45, 0.00) ( 0.00, 0.00) ( 0.00,-0.00)

```



000	TAUROD	1.20,	LAG	0.35,	THROTLAG	0.08,	TAUENG	0.08,	DELAY	0.00,	KFM	1.00
008	TAUROD	1.20,	LAG	0.35,	THROTLAG	0.08,	TAUENG	0.08,	DELAY	0.18,	KFM	1.00
012	TAUROD	1.20,	LAG	0.35,	THROTLAG	0.08,	TAUENG	0.08,	DELAY	0.28,	KFM	1.00
016	TAUROD	1.20,	LAG	0.35,	THROTLAG	0.08,	TAUENG	0.08,	DELAY	0.37,	KFM	1.00
024	TAUROD	1.20,	LAG	0.35,	THROTLAG	0.08,	TAUENG	0.08,	DELAY	0.55,	KFM	1.00
032	TAUROD	1.20,	LAG	0.35,	THROTLAG	0.08,	TAUENG	0.08,	DELAY	0.74,	KFM	1.00
040	TAUROD	1.20,	LAG	0.35,	THROTLAG	0.08,	TAUENG	0.08,	DELAY	0.92,	KFM	1.00

CASE

Fig. D4 Performance and roots vs DELAY for TAUROD = 1.2.

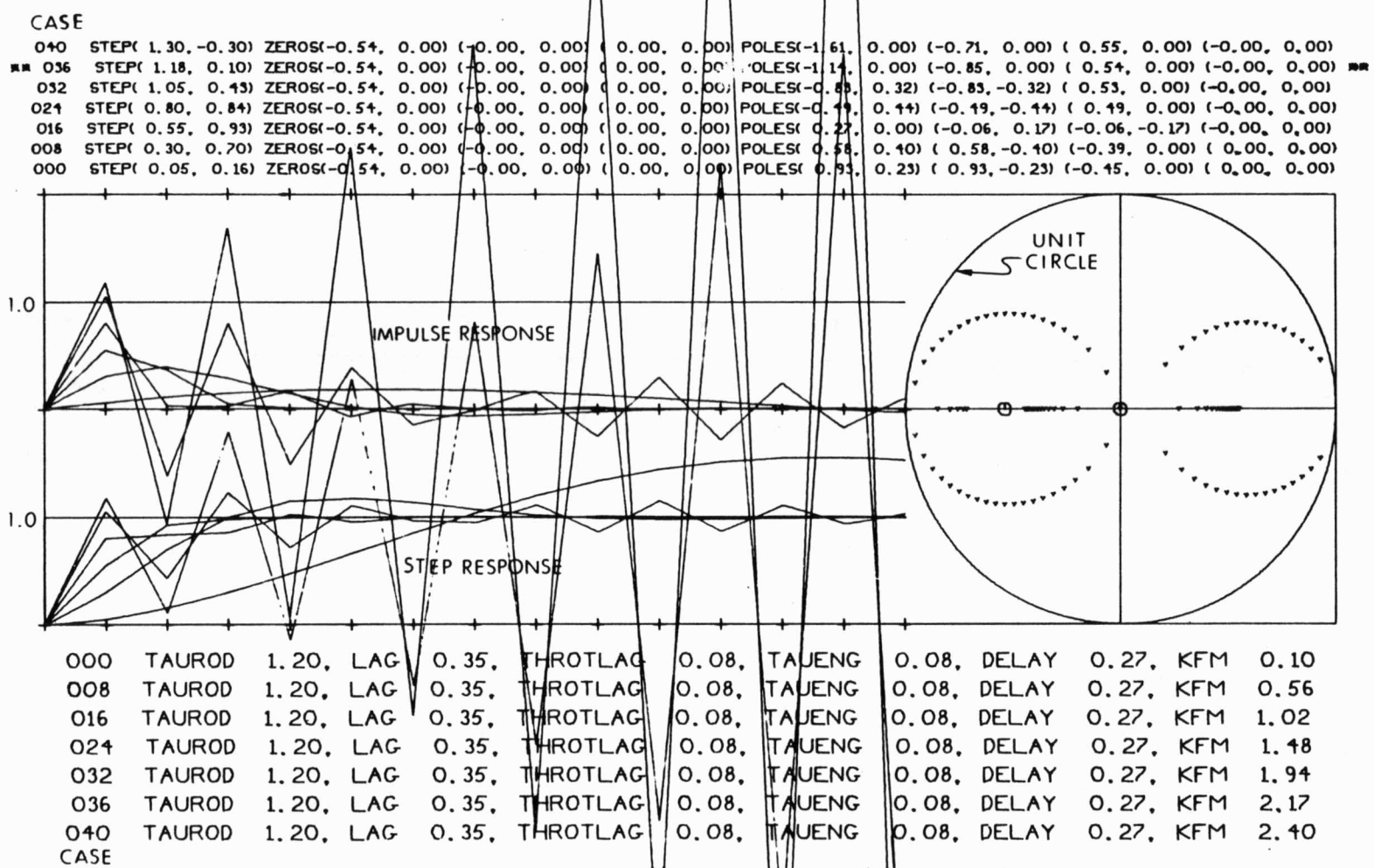


Fig. D5 Performance and roots vs KFM for TAUROD = 1.2.

	INITIAL VALUE	LAST UNSTABLE VALUE	FIRST STABLE VALUE	LAST STABLE VALUE	FIRST UNSTABLE VALUE	FINAL VALUE
TAUROD	1.0	X	X	X	X	1.0
LAG	-1.2	- .686	- .622	.792	.856	1.37
THROTLAG	- .41	- .294	- .275	.264	.283	.36
TAUENG	0	X	X	.581	.604	.93
DELAY	0	X	X	X	X	.92
KFM	.1	X	X	1.88	1.94	2.4

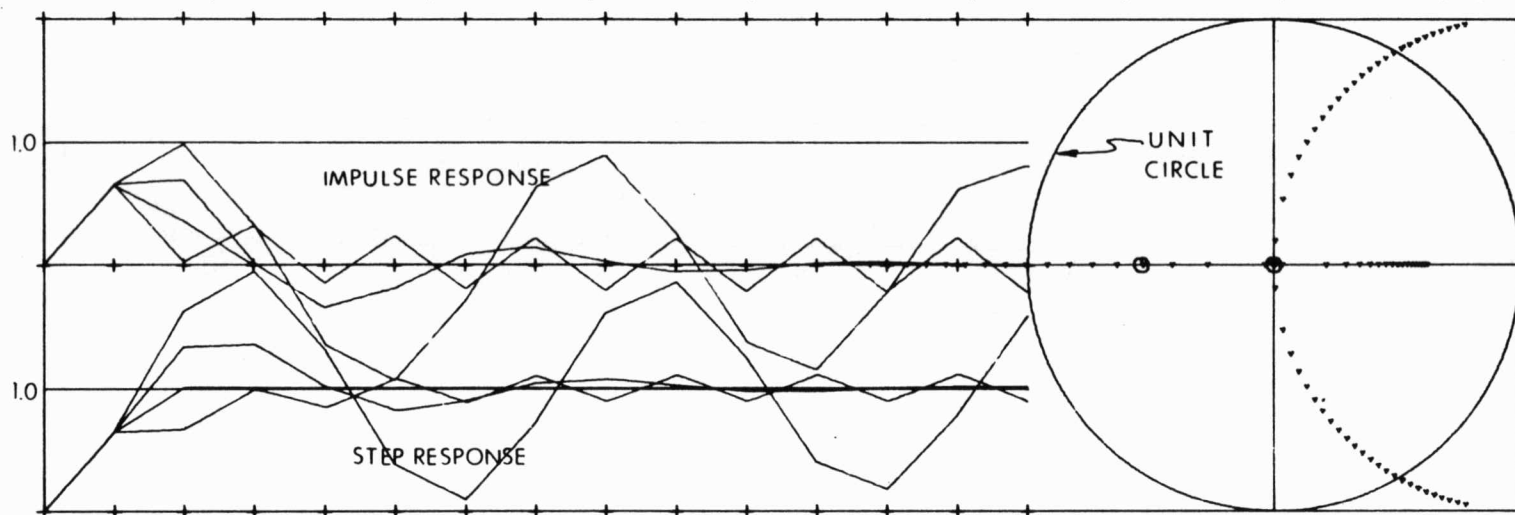
Table D2 STABILITY REGIONS OF EACH PARAMETER FOR TAUROD=1.0

CASE

```

040 STEP( 0.65, 0.34) ZEROS(-0.54, 0.00) (-0.00, 0.00) ( 0.00, 0.00) POLES(-1.64, 0.00) ( 0.62, 0.00) ( 0.00, 0.00) ( 0.00,-0.00)
■ 032 STEP( 0.65, 0.67) ZEROS(-0.54, 0.00) (-0.00, 0.00) ( 0.00, 0.00) POLES(-1.01, 0.00) ( 0.50, 0.00) ( 0.00, 0.01) ( 0.00,-0.01) ■
024 STEP( 0.65, 1.01) ZEROS(-0.54, 0.00) (-0.00, 0.00) ( 0.00, 0.00) POLES( 0.01, 0.10) ( 0.01,-0.10) (-0.04, 0.00) ( 0.03, 0.00)
016 STEP( 0.65, 1.34) ZEROS(-0.54, 0.00) (-0.00, 0.00) ( 0.00, 0.00) POLES( 0.26, 0.67) ( 0.26,-0.67) (-0.00, 0.00) ( 0.00, 0.00)
■ 009 STEP( 0.65, 1.63) ZEROS(-0.54, 0.00) (-0.00, 0.00) ( 0.00, 0.00) POLES( 0.49, 0.86) ( 0.49,-0.86) (-0.00, 0.00) ( 0.00, 0.00) ■
008 STEP( 0.65, 1.67) ZEROS(-0.54, 0.00) (-0.00, 0.00) ( 0.00, 0.00) POLES( 0.52, 0.88) ( 0.52,-0.88) (-0.00, 0.00) ( 0.00, 0.00)
000 STEP( 0.65, 2.01) ZEROS(-0.54, 0.00) (-0.00, 0.00) ( 0.00, 0.00) POLES( 0.77, 0.97) ( 0.77,-0.97) ( 0.00, 0.00) ( 0.00,-0.00)

```



```

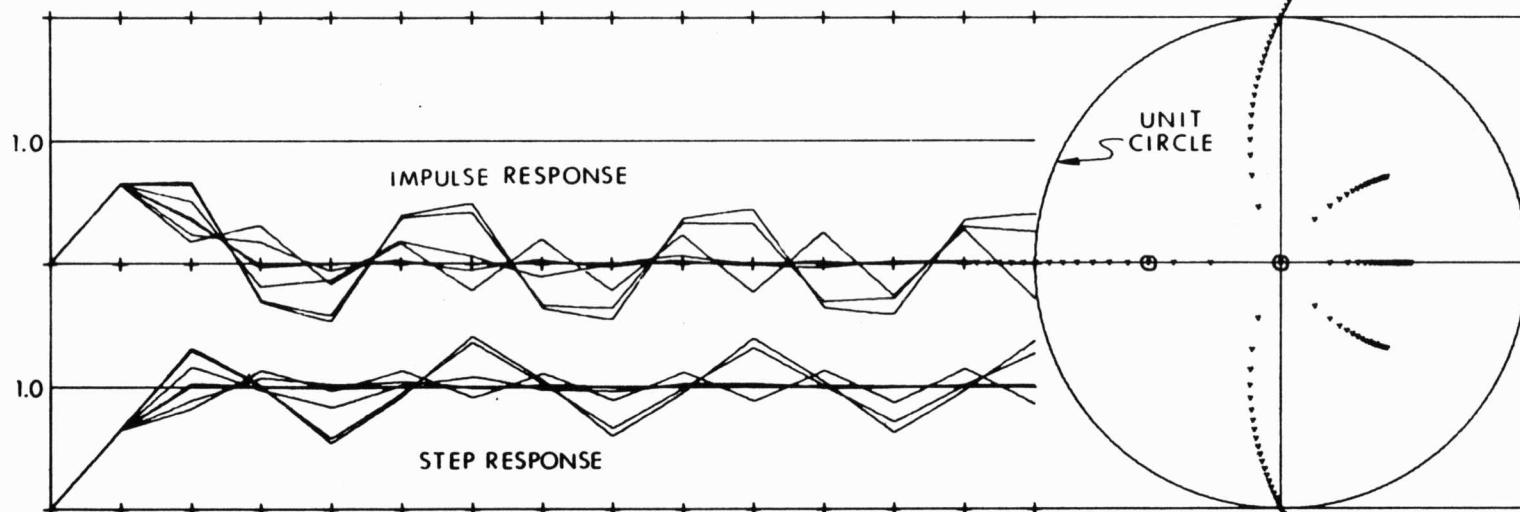
000 TAUROD 1.00, LAG -1.20, THROTLAG 0.08, TAUENG 0.08, DELAY 0.27, KFM 1.00
008 TAUROD 1.00, LAG -0.69, THROTLAG 0.08, TAUENG 0.08, DELAY 0.27, KFM 1.00
009 TAUROD 1.00, LAG -0.62, THROTLAG 0.08, TAUENG 0.08, DELAY 0.27, KFM 1.00
016 TAUROD 1.00, LAG -0.17, THROTLAG 0.08, TAUENG 0.08, DELAY 0.27, KFM 1.00
024 TAUROD 1.00, LAG 0.34, THROTLAG 0.08, TAUENG 0.08, DELAY 0.27, KFM 1.00
032 TAUROD 1.00, LAG 0.86, THROTLAG 0.08, TAUENG 0.08, DELAY 0.27, KFM 1.00
040 TAUROD 1.00, LAG 1.37, THROTLAG 0.08, TAUENG 0.08, DELAY 0.27, KFM 1.00

```

CASE

Fig. D6 Performance and roots vs LAG for TAUROD = 1.0.

CASE
 040 STEP(0.65, 0.75) ZEROS(-0.54, 0.00) (-0.00, 0.00) (0.00, 0.00) POLES(-1.24, 0.00) (0.43, 0.35) (0.43,-0.35) (0.00, 0.00)
 036 STEP(0.65, 0.82) ZEROS(-0.54, 0.00) (-0.00, 0.00) (0.00, 0.00) POLES(-1.05, 0.00) (0.39, 0.33) (0.39,-0.33) (0.00, 0.00) ■■
 032 STEP(0.65, 0.89) ZEROS(-0.54, 0.00) (-0.00, 0.00) (0.00, 0.00) POLES(-0.83, 0.00) (0.33, 0.31) (0.33,-0.31) (0.00, 0.00)
 025 STEP(0.65, 1.01) ZEROS(-0.54, 0.00) (-0.00, 0.00) (0.00, 0.00) POLES(-0.09, 0.23) (-0.09,-0.23) (0.20, 0.00) (-0.00, 0.00)
 024 STEP(0.65, 1.02) ZEROS(-0.54, 0.00) (-0.00, 0.00) (0.00, 0.00) POLES(-0.12, 0.35) (-0.12,-0.35) (0.27, 0.00) (-0.00, 0.00)
 016 STEP(0.65, 1.16) ZEROS(-0.54, 0.00) (-0.00, 0.00) (0.00, 0.00) POLES(-0.09, 0.75) (-0.09,-0.75) (0.43, 0.00) (-0.00, 0.00)
 008 STEP(0.65, 1.29) ZEROS(-0.54, 0.00) (-0.00, 0.00) (0.00, 0.00) POLES(-0.02, 0.96) (-0.02,-0.96) (0.49, 0.00) (-0.00, 0.00)
 ■ 007 STEP(0.65, 1.31) ZEROS(-0.54, 0.00) (-0.00, 0.00) (0.00, 0.00) POLES(-0.01, 0.98) (-0.01,-0.98) (0.50, 0.00) (-0.00, 0.00) ■
 000 STEP(0.65, 1.43) ZEROS(-0.54, 0.00) (-0.00, 0.00) (0.00, 0.00) POLES(0.07, 1.12) (0.07,-1.12) (0.53, 0.00) (-0.00, 0.00)



000	TAUROD	1.00,	LAG	0.35,	THROTLAG	-0.41,	TAUENG	0.08,	DELAY	0.27,	KFM	1.00
007	TAUROD	1.00,	LAG	0.35,	THROTLAG	-0.28,	TAUENG	0.08,	DELAY	0.27,	KFM	1.00
008	TAUROD	1.00,	LAG	0.35,	THROTLAG	-0.26,	TAUENG	0.08,	DELAY	0.27,	KFM	1.00
016	TAUROD	1.00,	LAG	0.35,	THROTLAG	-0.10,	TAUENG	0.08,	DELAY	0.27,	KFM	1.00
024	TAUROD	1.00,	LAG	0.35,	THROTLAG	0.05,	TAUENG	0.08,	DELAY	0.27,	KFM	1.00
025	TAUROD	1.00,	LAG	0.35,	THROTLAG	0.07,	TAUENG	0.08,	DELAY	0.27,	KFM	1.00
032	TAUROD	1.00,	LAG	0.35,	THROTLAG	0.21,	TAUENG	0.08,	DELAY	0.27,	KFM	1.00
036	TAUROD	1.00,	LAG	0.35,	THROTLAG	0.28,	TAUENG	0.08,	DELAY	0.27,	KFM	1.00
040	TAUROD	1.00,	LAG	0.35,	THROTLAG	0.36,	TAUENG	0.08,	DELAY	0.27,	KFM	1.00

CASE

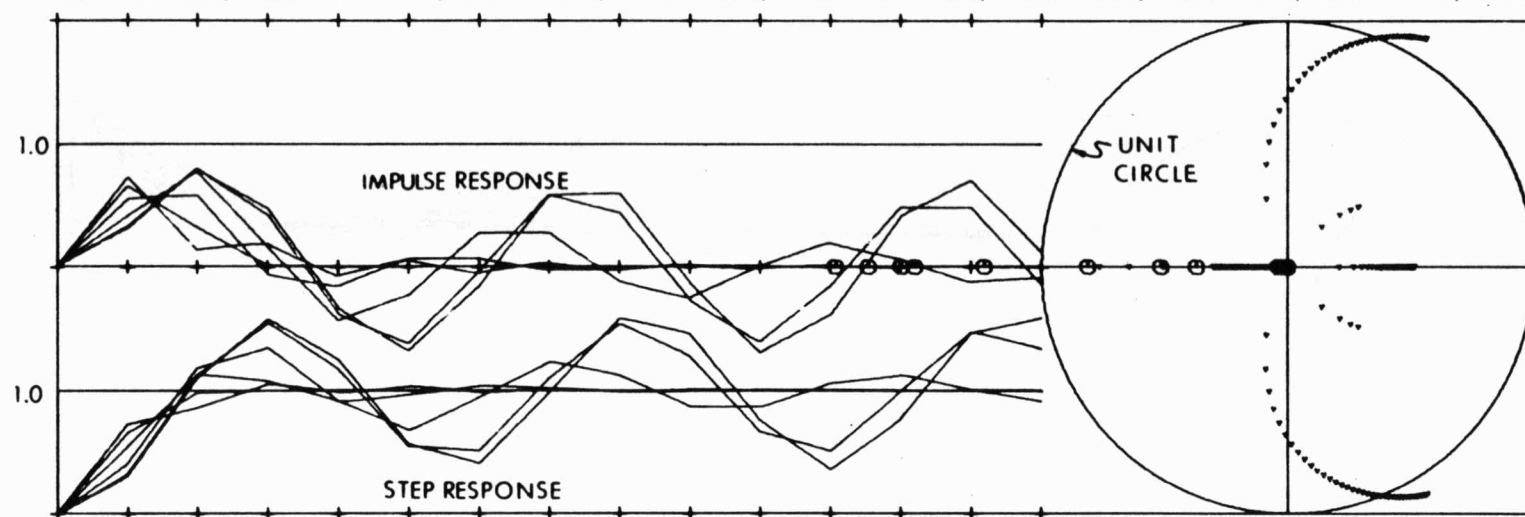
Fig. D7 Performance and roots vs THROTLAG for TAUROD = 1.0.

CASE

```

040 STEP( 0.22, 0.94) ZEROS(-1.84, 0.00) (-0.04, 0.00) ( 0.00, 0.00) POLES( 0.56, 0.92) ( 0.56, -0.92) ( 0.52, 0.00) (-0.30, 0.00)
032 STEP( 0.26, 1.03) ZEROS(-1.70, 0.00) (-0.03, 0.00) ( 0.00, 0.00) POLES( 0.47, 0.93) ( 0.47, -0.93) ( 0.49, 0.00) (-0.26, 0.00)
■■ 026 STEP( 0.31, 1.10) ZEROS(-1.57, 0.00) (-0.03, 0.00) ( 0.00, 0.00) POLES( 0.38, 0.93) ( 0.38, -0.93) ( 0.47, 0.00) (-0.23, 0.00) ■■
024 STEP( 0.32, 1.12) ZEROS(-1.52, 0.00) (-0.03, 0.00) ( 0.00, 0.00) POLES( 0.34, 0.92) ( 0.34, -0.92) ( 0.47, 0.00) (-0.21, 0.00)
016 STEP( 0.41, 1.18) ZEROS(-1.23, 0.00) (-0.02, 0.00) ( 0.00, 0.00) POLES( 0.17, 0.86) ( 0.17, -0.86) ( 0.12, 0.00) (-0.13, 0.00)
008 STEP( 0.55, 1.13) ZEROS(-0.81, 0.00) (-0.00, 0.00) ( 0.00, 0.00) POLES(-0.03, 0.63) (-0.03, -0.63) ( 0.34, 0.00) (-0.03, 0.00)
003 STEP( 0.66, 0.98) ZEROS(-0.51, 0.00) (-0.00, 0.00) ( 0.00, 0.00) POLES(-0.30, 0.00) ( 0.14, 0.16) ( 0.14, -0.16) ( 0.00, 0.00)
000 STEP( 0.73, 0.86) ZEROS(-0.37, 0.00) ( 0.00, 0.00) ( 0.00, 0.00) POLES(-0.76, 0.00) ( 0.29, 0.24) ( 0.29, -0.24) ( 0.00, 0.00)

```



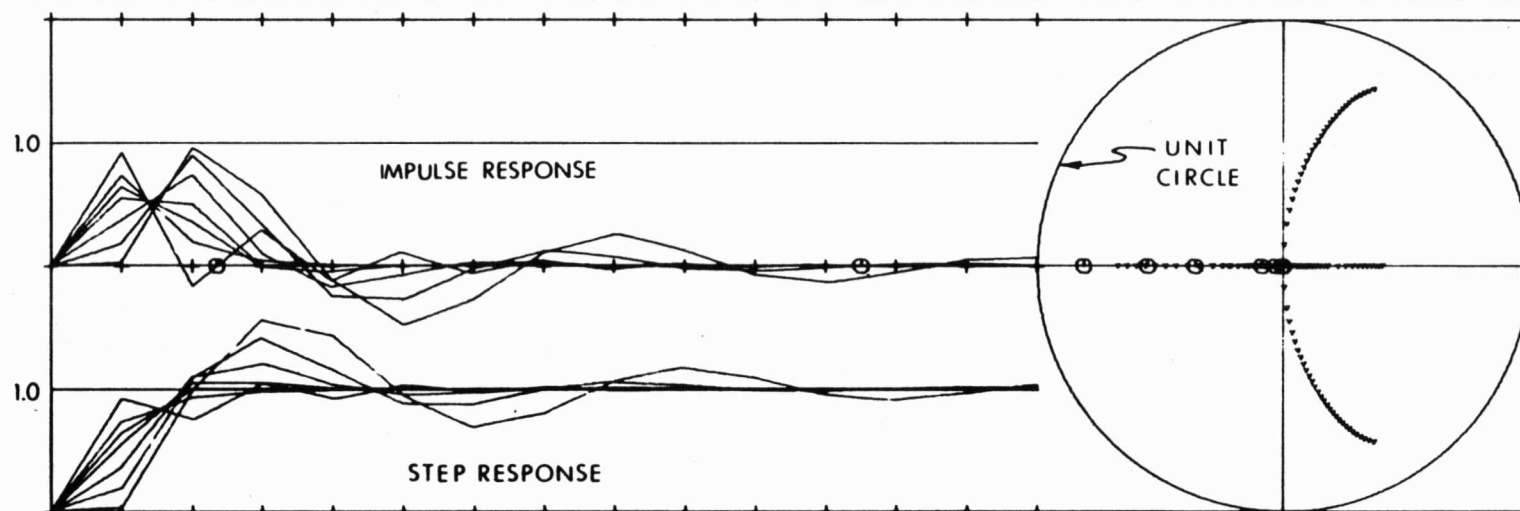
000	TAUROD	1.00,	LAG	0.35,	THROTLAG	0.08,	TAUENG	0.00,	DELAY	0.27,	KFM	1.00
003	TAUROD	1.00,	LAG	0.35,	THROTLAG	0.08,	TAUENG	0.07,	DELAY	0.27,	KFM	1.00
008	TAUROD	1.00,	LAG	0.35,	THROTLAG	0.08,	TAUENG	0.19,	DELAY	0.27,	KFM	1.00
016	TAUROD	1.00,	LAG	0.35,	THROTLAG	0.08,	TAUENG	0.37,	DELAY	0.27,	KFM	1.00
024	TAUROD	1.00,	LAG	0.35,	THROTLAG	0.08,	TAUENG	0.56,	DELAY	0.27,	KFM	1.00
026	TAUROD	1.00,	LAG	0.35,	THROTLAG	0.08,	TAUENG	0.60,	DELAY	0.27,	KFM	1.00
032	TAUROD	1.00,	LAG	0.35,	THROTLAG	0.08,	TAUENG	0.74,	DELAY	0.27,	KFM	1.00
040	TAUROD	1.00,	LAG	0.35,	THROTLAG	0.08,	TAUENG	0.93,	DELAY	0.27,	KFM	1.00

CASE

Fig. D8 Performance and roots vs TAUENG for TAUROD = 1.0.

CASE

040 STEP(0.03, 0.99) ZEROS(81.11, 0.00) (-0.03, 0.00) (0.00, 0.00) POLES(0.37, 0.72) (0.37, -0.72) (-0.34, 0.00) (0.18, 0.00)
032 STEP(0.19, 1.08) ZEROS(-4.33, 0.00) (-0.00, 0.00) (0.00, 0.00) POLES(0.24, 0.64) (0.24, -0.64) (-0.10, 0.00) (0.08, 0.00)
024 STEP(0.37, 1.10) ZEROS(-1.71, 0.00) (-0.00, 0.00) (0.00, 0.00) POLES(0.14, 0.51) (0.14, -0.51) (-0.04, 0.00) (0.04, 0.00)
016 STEP(0.55, 1.05) ZEROS(-0.81, 0.00) (-0.00, 0.00) (0.00, 0.00) POLES(0.05, 0.31) (0.05, -0.31) (-0.02, 0.00) (0.02, 0.00)
012 STEP(0.64, 1.00) ZEROS(-0.55, 0.00) (-0.00, 0.00) (0.00, 0.00) POLES(0.01, 0.09) (0.01, -0.09) (-0.04, 0.00) (0.04, 0.00)
008 STEP(0.74, 0.94) ZEROS(-0.36, 0.00) (-0.00, 0.00) (0.00, 0.00) POLES(-0.34, 0.00) (0.25, 0.00) (0.00, 0.01) (0.00, -0.01)
000 STEP(0.92, 0.75) ZEROS(-0.09, 0.00) (0.00, 0.00) (0.00, 0.00) POLES(-0.67, 0.00) (0.40, 0.00) (0.00, 0.00) (0.00, -0.00)



000 TAUROD 1.00, LAG 0.35, THROTLAG 0.08, TAUENG 0.08, DELAY 0.00, KFM 1.00
008 TAUROD 1.00, LAG 0.35, THROTLAG 0.08, TAUENG 0.08, DELAY 0.18, KFM 1.00
012 TAUROD 1.00, LAG 0.35, THROTLAG 0.08, TAUENG 0.08, DELAY 0.28, KFM 1.00
016 TAUROD 1.00, LAG 0.35, THROTLAG 0.08, TAUENG 0.08, DELAY 0.37, KFM 1.00
024 TAUROD 1.00, LAG 0.35, THROTLAG 0.08, TAUENG 0.08, DELAY 0.55, KFM 1.00
032 TAUROD 1.00, LAG 0.35, THROTLAG 0.08, TAUENG 0.08, DELAY 0.74, KFM 1.00
040 TAUROD 1.00, LAG 0.35, THROTLAG 0.08, TAUENG 0.08, DELAY 0.92, KFM 1.00

CASE

Fig. D9 Performance and roots vs DELAY for TAUROD = 1.0.

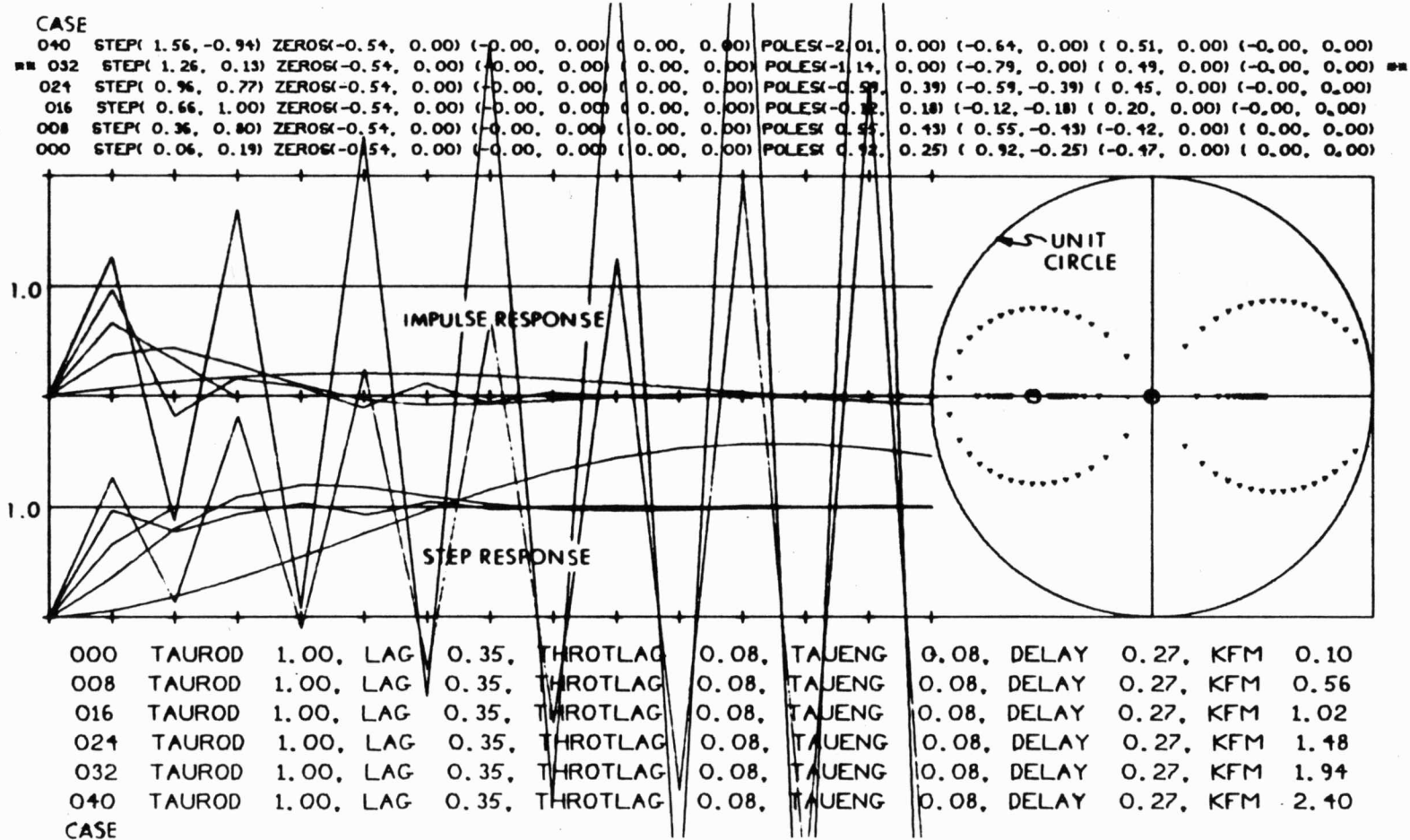


Fig. D10 Performance and roots vs KFM for TAUROD = 1.0.

DISTRIBUTION LIST

D. Hoag	T. Fitzgibbon	T. Brand
W. Stameris	A. Klumpp (25)	J. Kernan
N. Sears	B. Kriegsman	A. Engel
L. Larson	E. Muller	B. McCoy
R. Battin	D. Moore	R. Schlundt
G. Stubbs	R. Gilbert (KSC)	G. Kalan (25)
G. Silver	R. Bairnsfather	D. Keene
J. Gilmore	J. Jones	R. Stengel
G. Ogletree	P. Maybeck	E. Olsson
P. Felleman	A. Penchuk	I. Johnson
T. Lawton (MSC)	J. Turnbull	A. Woodin
R. O'Donnell (KSC)	J. Speyer	R. Metzinger
J. Vittek	P. Weissman	J. O'Connor
M. Johnson	T. Edelbaum	R. McKern
G. Cherry	R. Ragan	L.B. Johnson
R. Larson	J. Scanlon	W. Tanner
S. Copps	D. Eyles	R. White
G. Levine	M. Johnston	P. Mimno
M. Hamilton	D. Gustafson	K. Glick
D. Fraser	C. Pu	R. Weatherbee
J. Nevins	W. Robertson	Apollo Library (2) CSDL/TDC (10)

External:

NASA/RASPO	(1)
AC Electronics	(3)
Kollsman	(2)
Raytheon	(2)
MSC:	(27&1R)

National Aeronautics and Space Administration
Manned Spacecraft Center
Houston, Texas 77058

ATTN: Apollo Document Control Group (BM 86) (18&1R)
M. Holley (2)
T. Gibson (1)
J. Suddath (1)
J. Alphin (1)
C. Hackler (1)
K. Cox (1)
W. Tindall (1)
J. Garman (1)

KSC: (2&1R)

National Aeronautics and Space Administration
J. F. Kennedy Space Center
J. F. Kennedy Space Center, Florida 32899
ATTN: Technical Document Control Office
C. Floyd (1)
B. Pearson (1)

LCR: (2)

National Aeronautics and Space Administration
Langley Research Center
Hampton, Virginia
ATTN: Mr. A. T. Mattson

GA: (5&1R)

Grumman Aerospace Corporation
Data Operations and Services, Plant 25
Bethpage, Long Island, New York
ATTN: Mr. E. Stern (3&1R)
Mr. C. Tillman (1)
Mr. R. Schindwolf (1)

NAR: (8&1R)

North American Rockwell, Inc.
Space Division
12214 Lakewood Boulevard
Downey, California 90241
ATTN: CSM Data Management
D/096-402 AE99

NAR RASPO: (1)

NASA Resident Apollo Spacecraft Program Office
North American Rockwell, Inc.
Space Division
12214 Lakewood Boulevard
Downey, California 90241

GE: (1)

General Electric Company
Apollo Systems
P. O. Box 2500
Daytona Beach, Florida 32015
ATTN: E. P. Padgett, Jr./Unit 509

BELLCOMM: (9)

Bellcomm Inc.
1100 17th Street N. W.
Washington, D.C. 20036
ATTN: Info. Analysis Section (6)
J. Sorensen (1)
T. Hoekstra (1)
W. Heffron (1)

TRW: (7)

TRW Systems Group
Bldg 82 Room 2045
One Space Park
Redondo Beach, California 90278
ATTN: H. V. Kienberger (5)
R. Seto (1)
R. Lee (1)